Contrib Mineral Petrol (2006) 152:399–419
DOI 10.1007/s00410-006-0115-2

ORIGINAL PAPER

The stability of primary alluaudites in granitic pegmatites: an experimental investigation of the $Na_2(Mn_{2-2x}Fe_{1+2x})(PO_4)_3$ system

Frédéric Hatert · André-Mathieu Fransolet ·
Walter V. Maresch

Received: 6 January 2006 / Accepted: 5 June 2006 / Published online: 8 August 2006

Abstract In order to assess the geothermometric potential of the $Na_2(Mn_{2-2x}Fe_{1+2x})(PO_4)_3$ system (x = 0–1), which represents the compositions of natural weakly oxidized alluaudites, we performed hydrothermal experiments between 400 and 800°C, at 1 kbar, under an oxygen fugacity ($f(O_2)$) controlled by the Ni–NiO (NNO), Fe_2O_3–Fe_3O_4 (HM), Cu_2O–CuO (CT), and Fe–Fe_3O_4 (MI) buffers. When $f(O_2)$ is controlled by NNO, single-phase alluaudites crystallize at 400 and 500°C, whereas the association alluaudite + marićite appears between 500 and 700°C. The limit between these two fields corresponds to the maximum temperature that can be reached by alluaudites in granitic pegmatites, because marićite has never been observed in these geological environments. Because alluaudites are very sensitive to variations of oxygen fugacity, the field of hagendorfite, $Na_2MnFe^{2+}Fe^{3+}(PO_4)_3$, has been positioned in the $f(O_2)$–T diagram, and provides a tool that can be used to estimate the oxygen fugacity conditions that prevailed in granitic pegmatites during the crystallization of this phosphate.

Communicated by J. Hoefs

F. Hatert (✉) · A.-M. Fransolet
Laboratoire de Minéralogie, Département de Géologie,
Bâtiment B18, Université de Liège,
4000 Sart-Tilman, Belgium
e-mail: fhatert@ulg.ac.be

W. V. Maresch
Institut für Geologie, Mineralogie und Geophysik,
Ruhr-Universität Bochum, 44780 Bochum, Germany

Keywords Primary alluaudites · Na–Mn–Fe^{2+}–Fe^{3+} phosphates · Phase relations · Petrological implications · Pegmatites

Introduction

The alluaudite mineral group consists of Na–Mn–Fe-bearing phosphates which are known to occur in granitic pegmatites, particularly in the beryl-columbite-phosphate subtype of the rare-element pegmatites, according to the classification of Černý (1991). In granitic pegmatites, alluaudite-group minerals exhibit chemical compositions ranging from $Na_2Mn(Fe^{2+}Fe^{3+})(PO_4)_3$ to $\square NaMnFe_2^{3+}(PO_4)_3$, with Mn^{2+} or some Ca^{2+} replacing Na^+, Fe^{2+} replacing Mn^{2+}, and some Mg^{2+} or Mn^{2+} replacing iron, where □ represents a lattice vacancy.

According to Moore (1971), alluaudites are produced from primary phosphates of the triphylite–lithiophilite series, $LiFe^{2+}(PO_4)$–$LiMn(PO_4)$, by oxidation coupled with a Li → Na metasomatic exchange process. Alluaudite-group minerals, which are generally very fine grained compared to minerals of the triphylite–lithiophilite series, were consequently considered to be of secondary origin. Several occurrences of such secondary alluaudites, produced from triphylite–lithiophilite or from their oxidation products ferrisicklerite–sicklerite, $Li_{1-x}(Fe^{3+},Mn^{2+})(PO_4)$–$Li_{1-x}(Mn^{2+},Fe^{3+})(PO_4)$, and heterosite–purpurite, $(Fe^{3+},Mn^{3+})(PO_4)$–$(Mn^{3+},Fe^{3+})(PO_4)$, were reported by Huvelin et al. (1972), Fransolet (1975), Fontan et al. (1976), Fontan (1978), Boury (1981), Lahti (1981), Fransolet et al. (1985, 1986), Keller and Von Knorring (1989), Roda et al. (1996), and Roda Robles et al. (1998).

The existence of primary alluaudites was first mentioned by Quensel (1957), who considered that hühnerkobelite and varulite crystallized between 400 and 600°C, during the first stages of pegmatite evolution [hühnerkobelite is not a valid species any more, and corresponds to alluaudite or ferroalluaudite, according to Moore and Ito (1979)]. Fransolet (1975, 1977) noted sharp contacts between alluaudite and ferrisicklerite from the Buranga pegmatite, Rwanda, without any replacement texture. This observation indicates that the metasomatic replacement process proposed by Moore (1971) cannot be generalized. Héreng (1989) re-examined the samples from the Buranga pegmatite, and observed three different primary parageneses: alluaudite + triphylite, alluaudite + fillowite, and alluaudite + arrojadite. The large size of the alluaudite grains from the Buranga pegmatite, which can reach 1 cm in length, is also a good argument for distinguishing primary from secondary fine-grained alluaudites. More recently, Fransolet et al. (1994, 1997, 1998, 2004) observed several parageneses involving primary alluaudites: alluaudite + arrojadite in Hagendorf-Süd, Germany; alluaudite + fillowite in Rusororo, Rwanda, and Kabira, Uganda; alluaudite + ferrisicklerite + heterosite in Kibingo and Wasurenge, Rwanda.

As observed for the phosphates of the triphylite–lithiophilite series, which progressively transform to ferrisicklerite–sicklerite and to heterosite–purpurite due to oxidation and Li-leaching, the primary alluaudites, which are weakly oxidized, progressively transform into oxidized secondary alluaudites. In order to maintain charge balance, Na is leached out of the alluaudite structure, according to the substitution mechanism $Na^+ + Fe^{2+} \rightarrow \square + Fe^{3+}$, as observed by Mason (1941) and Fransolet et al. (1985, 1986, 2004). This oxidation mechanism, coupled with Na leaching, explains the transformation of hagendorfite, $Na_2MnFe^{2+}Fe^{3+}(PO_4)_3$, into alluaudite, $\square NaMnFe^{3+}_2(PO_4)_3$, and of ferrohagendorfite, $Na_2Fe^{2+}_2Fe^{3+}(PO_4)_3$, into ferroalluaudite, $\square NaFe^{2+}Fe^{3+}_2(PO_4)_3$.

In the genetic processes affecting Fe–Mn phosphates in granitic pegmatites, minerals of the alluaudite group occupy a crucial position. Due to their flexible crystal structure, which is able to accommodate Fe^{2+} and Fe^{3+} in variable amounts, alluaudites are very stable and crystallize from the first stages of pegmatite evolution to the latest oxidation processes. Since the petrogenetic importance of accessory phosphates has been demonstrated in the ultrahigh-pressure rocks of the Dora-Maira massif (Brunet et al. 1998), it now clearly appears that experimental studies on these rare minerals are necessary to better understand the genesis of granitic pegmatites (London et al. 1999, 2001). With this goal in mind, we decided to assess the geothermometric potential of the $Na_2(Mn_{2-2x}Fe_{1+2x})(PO_4)_3$ system (x = 0–1), which models the compositions of natural, weakly oxidized, primary alluaudites. For this purpose, we performed systematic hydrothermal experiments between 400 and 800°C, at 1 kbar and under oxygen fugacities controlled by the Ni–NiO, Fe_2O_3–Fe_3O_4, Cu_2O–CuO, and Fe–Fe_3O_4 buffers. The aim of this paper is to report the results of these experiments, which will provide a tool for constraining the temperature and oxygen fugacity conditions that prevailed in granitic pegmatites during the crystallization of alluaudites.

Previous studies

Crystal structure, chemical composition, and nomenclature of natural alluaudites

By using a single crystal from the Buranga pegmatite, Rwanda, Moore (1971) determined the crystal structure of alluaudite in the monoclinic *C2/c* space group, and proposed the general structural formula $X(2)X(1)M(1)M(2)_2(PO_4)_3$, with Z = 4. The structure consists of kinked chains of edge-sharing octahedra stacked parallel to {101}. These chains are formed by a succession of $M(2)$ octahedral pairs linked by highly distorted $M(1)$ octahedra. Equivalent chains are connected in the *b* direction by the $P(1)$ and $P(2)$ phosphate tetrahedra to form sheets oriented perpendicular to [010]. These interconnected sheets produce channels parallel to the *c* axis, channels which contain the distorted cubic $X(1)$ site and the four-coordinated $X(2)$ site (Fig. 1).

According to Moore (1971), the cations are distributed among the different crystallographic sites as a function of their ionic radii. Accordingly, the large $X(2)$ site contains Na, K and vacancies; $X(1)$ contains Na, Mn, and Ca; $M(1)$ contains Mn and Fe^{2+}; and the small $M(2)$ site contains Fe^{3+}, Fe^{2+}, Mn, Mg, and Li. Because Mn dominates on the $M(1)$ site, and Fe^{2+} and Fe^{3+} dominate on the $M(2)$ site, Moore (1971) proposed the ideal formula $Na_2MnFe^{2+}Fe^{3+}(PO_4)_3$, from which the majority of natural alluaudites can be derived.

Moore and Ito (1979) investigated the crystal chemistry of several natural alluaudite samples, and also proposed a systematic nomenclature for the alluaudite group, which is based on the cation distribution among the different crystallographic sites. The mineral is given a generic name that depends on the

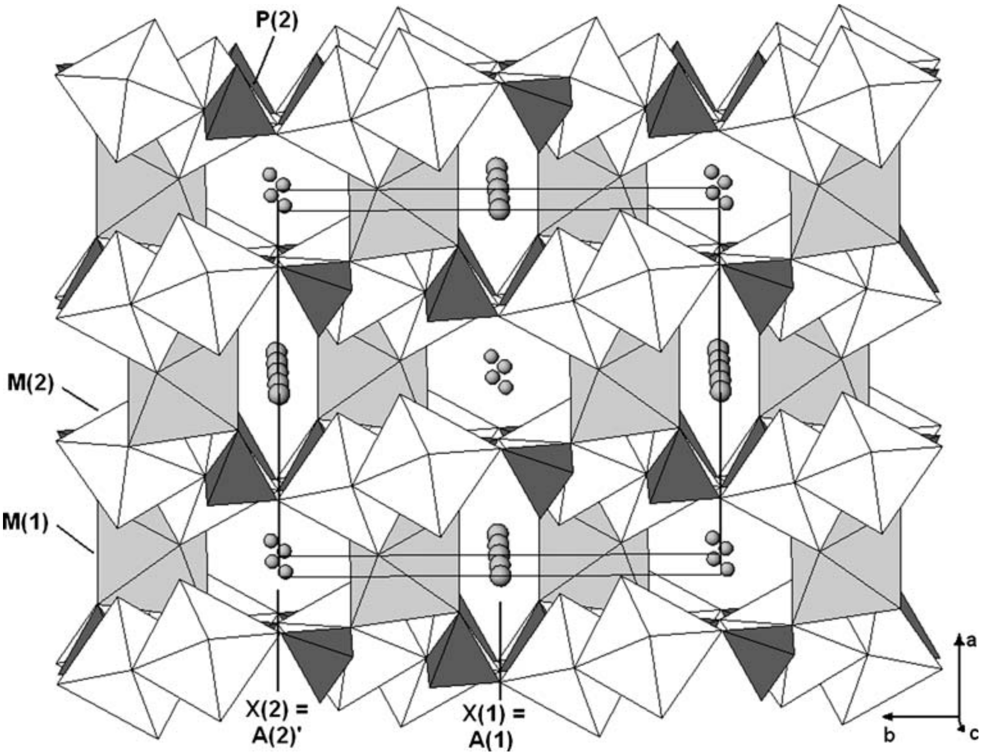

Fig. 1 A projection of the alluaudite structure. The PO_4 tetrahedra are densely shaded, the $M(1)$ octahedra are *shaded*, and the $M(2)$ octahedra are *unshaded*. The *circles* indicate Na at the $A(1)$ (= $X(1)$) and $A(2)'$ (= $X(2)$) crystallographic sites

predominant $M(2)$ content (Mn = varulite, Fe^{2+} = hagendorfite, Fe^{3+} = alluaudite), and characterized by a prefix reflecting the $M(1)$ content (Fe^{2+} = ferro-, and Mg = mag-). For example, the compositions $Na^{A2'}Na^{A1}(Fe^{2+})^{M1}(Fe^{2+}Fe^{3+})^{M2}(PO_4)_3$, $Na^{A2'}Na^{A1}(Mn)^{M1}(Fe^{2+}Fe^{3+})^{M2}(PO_4)_3$, and $Na^{A2'}Na^{A1}(Mn)^{M1}(MnFe^{3+})^{M2}(PO_4)_3$ correspond to the minerals ferrohagendorfite, hagendorfite and varulite, respectively, whereas the more oxidized compositions $\square^{A2'}Na^{A1}(Fe^{2+})^{M1}(Fe^{3+}Fe^{3+})^{M2}(PO_4)_3$ and $\square^{A2'}Na^{A1}(Mn)^{M1}(Fe^{3+}Fe^{3+})^{M2}(PO_4)_3$ correspond to ferroalluaudite and alluaudite, respectively (Fig. 2).

Crystal chemistry of synthetic alluaudite-type phosphates

Over the past 20 years, many phosphates, arsenates, molybdates, vanadates, and tungstates with the alluaudite structure have been synthesized (Auernhammer et al. 1993; Khorari 1997; Solodovnikov et al. 1998; Hatert et al. 2000a; Tsyrenova et al. 2000; Hatert 2002, 2004a; Redhammer et al. 2005). The structural investigation of these synthetic compounds showed the existence of new crystallographic sites localized in the channels of the structure, on positions which are different from those of $X(1)$ and $X(2)$. In order to take these new crystallographic sites into account, Hatert et al. (2000a) proposed the new general formula $[A(2)A(2)'][A(1)A(1)'A(1)''_2]M(1)M(2)_2[PO_4]_3$ for alluaudite-type compounds. In this formula, $A(1)$ and $A(2)'$ correspond to $X(1)$ and $X(2)$, respectively (Fig. 1). Except in some Cu- and H-bearing alluaudite-type compounds, the $A(1)'$, $A(1)''$, and $A(2)$ sites are empty (Hatert et al. 2000a).

In general, the cation distribution in synthetic alluaudite-type phosphates is controlled by the ionic radii of the cations, as suggested by Moore (1971) and Moore and Ito (1979). However, Li is surprisingly not localized on the small $M(2)$ crystallographic site, but rather on the large $A(1)$ site (Hatert et al. 2000a, 2002; Hatert 2004a), and a partially disordered distribution of cations with similar ionic radii has been observed in the compounds $Na_2Cd_2M^{3+}(PO_4)_3$ (M^{3+} = Ga, Fe^{3+}, Cr) (Antenucci 1992), $NaMn(Fe^{3+}{}_{1-x}In_x)_2(PO_4)_3$ (Hatert et al. 2003), $Na_{1.5}(Mn_{1-x}Cd_x)_{1.5}Fe^{3+}{}_{1.5}(PO_4)_3$ (Hatert 2002), and $Na_2(Mn_{1-x}Fe^{2+}{}_x)_2Fe^{3+}(PO_4)_3$ (Hatert et al. 2005).

Stability of highly oxidized alluaudites

The stability of highly oxidized alluaudites has been investigated experimentally by Hatert (2002, 2004b) and Hatert et al. (2000b), who have performed solid-state syntheses in the Na–Mn–Fe^{3+} (+ PO_4) system. In

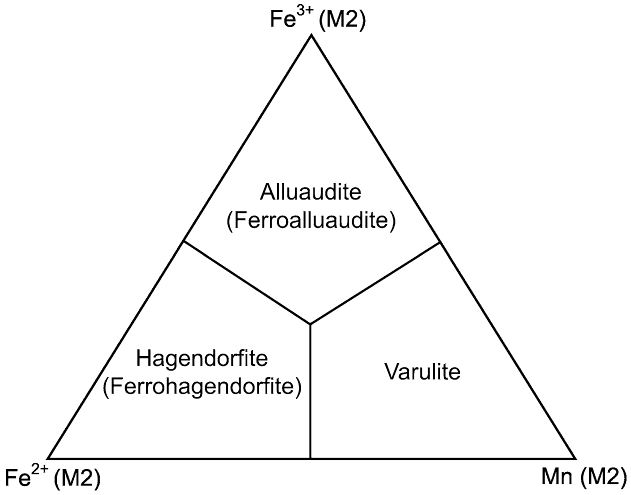

Fig. 2 Nomenclature of the alluaudite group of minerals, according to Moore and Ito (1979). When $M(1)$ is occupied by Mn, a generic name is given that depends on the predominant $M(2)$ content, and when $M(1)$ is occupied by Fe^{2+}, the prefix ferro- is added, leading to the names given in *parentheses*. A varulite with Fe^{2+} predominant on $M(1)$ is predicted to be unstable (Moore and Ito 1979), and the name "ferrohagendorfite" has been approved by the IMA-CNMMN without any formal species description. The name maghagendorfite corresponds to a hagendorfite where Mg is predominant on $M(1)$

the temperature range 850–950°C, at 1 bar and in air, alluaudites show a wide compositional field which covers more than 25% of the Na–Mn–Fe^{3+} (+ PO_4) ternary diagram surface. Some compositions of synthesized alluaudites are $NaMnFe^{3+}{}_2(PO_4)_3$, $Na_{1.5}Mn_{1.5}Fe^{3+}{}_{1.5}(PO_4)_3$, $Na_2Mn_2Fe^{3+}(PO_4)_3$, and $Mn_{2.25}Fe^{3+}{}_{1.5}(PO_4)_3$. The synthesis of these compounds indicates that the alluaudite-type structure is stable at high temperatures.

Starting from the $NaMnFe_2^{3+}(PO_4)_3$ nominal composition, the synthesis in air of an alluaudite-type compound with a chemical composition similar to that of alluaudite from the Buranga pegmatite, Rwanda, indicates that this natural oxidized alluaudite probably also crystallized under a very high oxygen fugacity. However, it is important to note that, even under the very high ambient oxygen fugacity conditions in these experiments, a small amount of Fe^{2+} occurs in this alluaudite-type compound, as shown by the Mössbauer spectral studies performed by Hermann et al. (2002) and Hatert et al. (2003, 2004). This amount of Fe^{2+}, which corresponds to ~ 19% of total iron, is necessary to stabilize the alluaudite structure, because the $M(2)$ crystallographic site is too large to be completely filled by the small Fe^{3+} cation, and must consequently contain a minimum of larger divalent cations (Hatert et al. 2000a, 2003).

Experimental procedure

The hydrothermal experiments were performed between 400 and 800°C at 1 kbar, starting from compositions $Na_2(Mn_{2-2x}Fe_{1+2x})(PO_4)_3$, with $x = 0.00$, 0.25, 0.50, 0.75, and 1.00. Stoichiometric quantities of $NaH_2PO_4{\cdot}H_2O$ (Merck, Darmstadt, Germany, min. 99%), $FePO_4$, MnO (Alfa, Karsruhe, Germany, 99.5%), and FeO (Aldrich, Steinheim, Germany, 99%) were homogenized in a mortar under acetone, in order to prevent oxidation of FeO. $FePO_4$ was previously synthesized by solid-state reaction in air, starting from a stoichiometric mixture of $NH_4H_2PO_4$ (Merck, min. 99%) and $FeSO_4{\cdot}7H_2O$ (Merck, min. 99.5%), which was heated in a platinum crucible at 900°C for 1 day.

Approximately 20–30 mg of the starting material were welded, together with 2 µl of distilled water, into small $Ag_{70}Pd_{30}$ tubes with an outer diameter of 2 mm, a wall thickness of 0.1 mm and a length of 25 mm. In order to control the oxygen fugacity, a double-capsule device similar to that developed by Eugster (1957) was used. Approximately 100–300 mg of oxygen fugacity buffer were introduced, together with 10 µl of distilled water, into large gold tubes of 4 mm outer diameter, 0.1 mm wall thickness, and 40 mm length. The $Ag_{70}Pd_{30}$ tubes were then placed in the larger gold tubes which were also welded. The oxygen fugacity buffers were homogeneous mixture of Ni + NiO (NNO, O'Neill and Pownceby 1993), Fe_2O_3 (hematite) + Fe_3O_4 (magnetite) (HM, Norton 1955), Cu_2O (cuprite) + CuO (tenorite) (CT, O'Neill 1988), and Fe (iron) + Fe_3O_4 (magnetite) (MI, O'Neill 1988).

The capsules were finally introduced into a conventional hydrothermal apparatus with horizontally arranged Tuttle-type cold-seal bombs (Tuttle 1949) for 3–12 days and then cooled in a stream of cold air. Pressure and temperature errors are estimated to be within ± 3% and ± 10°C, respectively. After the experiment, the buffer was examined by powder X-ray diffraction, in order to check if the mixture was still present. When the buffer was exhausted the results were not taken into account and a new experiment, with a larger amount of buffer and/or with a shorter duration, was performed.

The powder X-ray diffraction patterns of the synthesized compounds were recorded on a Philips PW-3710 diffractometer using 1.9373 Å FeK_α radiation. The unit-cell parameters were calculated with the LCLSQ 8.4 least-squares refinement program (Burnham 1991) from the d-spacings calibrated with $Pb(NO_3)_2$ as an internal standard.

Electron-microprobe analyses were performed with two Cameca SX-50 instruments located in Louvain-la-Neuve, Belgium (analyst J. Wautier), and in Toulouse, France (analysts F. Fontan and P. de Parseval), which operated in the wavelength-dispersion mode with an accelerating voltage of 15 kV and a beam current of 20 nA. The standards used in Louvain-la-Neuve were graftonite from Kabira (sample KF16, Fransolet 1975) (for Fe, Mn, P) and oligoclase (Na). In Toulouse, the standards were graftonite from Sidi-bou-Othmane (Fontan 1978) (for P), albite (Na), hematite (Fe), and synthetic $MnTiO_3$ (Mn). The formulae of alluaudite, "X-phase", and fillowite were calculated on the basis of 3, 4, and 6 P, respectively, and the FeO and Fe_2O_3 contents were then calculated to maintain charge balance. The alluaudite sample H.121 also necessitates the introduction of Mn_2O_3 to maintain charge balance. For marićite and $(Fe,Mn)_2P_2O_7$, that do not contain Fe^{3+}, iron was considered as FeO, and the formulae were then calculated on the basis of 4 and 7 O, respectively. The composition of hematite was calculated on the basis of two atoms, assuming that all iron was at the trivalent state. A careful examination of the analytical results (see below) shows that the different standards used significantly affect the general stoichiometry, with higher (Fe + Mn)/P and Na/P ratios in Toulouse. This underlines the crucial effect of standard choice on the analyses of phosphate minerals.

Phase characterization

Alluaudite-type phosphates

Alluaudite-type phosphates have been obtained in many experimental runs performed in this study, and they were frequently associated with other phases (Table 1), mainly marićite, "X-phase", and fillowite. At temperatures between 600 and 800°C, alluaudite sometimes crystallized in large crystals reaching 1 mm, showing a dark green to black color. These large crystals gave us the possibility to perform goniometric measurements, which indicate the presence of the forms {110}, {011} (Fig. 3a), {100} and {010}, sometimes associated with {021}, $\{\bar{1}11\}$ or $\{\bar{1}21\}$. Electron-microprobe analyses (Table 2) show a correlation between the number of vacancies per formula unit (pfu) and the number of Fe^{3+} pfu, in agreement with the substitution mechanism $Mn^{2+} + 2Fe^{2+} \rightarrow \square + 2Fe^{3+}$. established by Hatert (2004b). The unit-cell parameters of the alluaudite-type compounds synthesized in this study are given in Table 3.

The alluaudites synthesized below 600°C were generally very fine grained and, for this reason, no microprobe analyses were performed on these low-temperature runs. In order to estimate the $Fe_{total}/(Fe_{total} + Mn)$ ratio of alluaudite-type compounds, several correlations have therefore been established between this ratio and the unit-cell parameters (Fig. 4). Whereas the correlation coefficients R^2 are very good for the *a* and *b* parameters, as well as for the unit-cell volume, they show a weak correlation for *c* and *β*. The $Fe_{total}/(Fe_{total} + Mn)$ ratios of alluaudites synthesized at low temperatures, estimated with the correlations given in Fig. 4 for *a*, *b*, and *V*, are presented in Table 4.

Marićite-type phosphates

Marićite, $NaFe^{2+}(PO_4)$, is a phosphate mineral described by Sturman et al. (1977) from metamorphic phosphate nodules included in the schists of the Big Fish River area, Yukon, Canada. Le Page and Donnay (1977) described the crystal structure of this mineral, which has been hydrothermally synthesized by Bridson et al. (1998) between 200 and 250°C.

It is important to underline the differences between the crystal structures of marićite and that of natrophilite, $NaMn(PO_4)$, which is isostructural with olivine (Moore 1972). Whereas the space group *Pmnb* of these three minerals is identical, their unit-cell parameters are significantly different, with $a/b \sim 0.60$ for olivine-type compounds, and $a/b \sim 0.76$ for marićite-type compounds (Le Page and Donnay 1977). The marićite structure, more compact than the olivine structure, contains chains of edge-sharing *M*(1) octahedra, parallel to the *a* axis and occupied by Fe^{2+}. Each *M*(1) octahedron shares some faces with the *M*(2) polyhedra, which contain ten-coordinated Na. In the olivine structure, the *M*(1) chains are identical to those of marićite, but the *M*(2) octahedral sites are smaller than the *M*(2) sites of marićite, and only share one edge with the *M*(1) sites.

Synthetic natrophilite, $NaMn(PO_4)$, has been obtained by Engel (1976) at room temperature, whereas a marićite-type phosphate with the same composition was synthesized at 750°C. Engel (1976) consequently considers natrophilite to be a low-temperature polymorph of marićite. This conclusion is in good agreement with the observations of Moore (1972), who considers natural natrophilite as a secondary phosphate, produced from lithiophilite affected by a metasomatic Li → Na exchange process.

The hydrothermal experiments realized in the present study have shown the presence of marićite-type phosphates, frequently associated with alluaudites, between 500 and 800°C (Table 1). Marićite forms large colorless grains reaching 1 mm, with an irregular and frequently rounded shape (Fig. 3b). Identification has been performed by powder X-ray diffraction, and the

Table 1 Results of synthesis experiments on the $Na_2(Mn_{2-2x}Fe_{1+2x})(PO_4)_3$ starting compositions (x = 0, 0.25, 0.50, 0.75, 1)

Starting composition	*T* (°C)	*P* (kbar)	*f*(O_2)	Duration (days)	Run products	Run no.
$Na_2Mn_2Fe^{3+}(PO_4)_3$	400	1	NNO	6	Alluaudite + marićite (tr.)	H.082
	400	1	HM	3	Alluaudite	H.210
	500	1	NNO	7	Alluaudite + marićite	H.136
	500	1	HM	3	Alluaudite + marićite (tr.) ?	H.211
	600	1	NNO	6	Alluaudite + marićite + fillowite	H.076
	600	1	HM	6	Alluaudite + marićite + ? (tr.)	H.081
	600	1	CT	4	Alluaudite	H.109
	600	1	–	4	Alluaudite + marićite + filowite	H.114[a]
	700	1	NNO	7	X-phase + marićite + alluaudite	H.098
	700	1	HM	4	Alluaudite + marićite + ? (tr.)	H.199
	800	1	NNO	6	X-phase + alluaudite + marićite + fillowite	H.071
$Na_2Mn_{1,5}Fe^{2+}{}_{0,5}Fe^{3+}(PO_4)_3$	400	1	NNO	6	Alluaudite	H.083
	500	1	NNO	7	Alluaudite + marićite	H.137
	600	1	NNO	6	Alluaudite + marićite	H.077
	600	1	HM	4	Alluaudite	H.105
	600	1	CT	4	Alluaudite + hematite	H.110
	600	1	–	4	Alluaudite + marićite	H.115[a]
	700	1	NNO	7	Alluaudite + marićite	H.099
	700	1	HM	3	Alluaudite	H.213
	800	1	NNO	6	X-phase + marićite + alluaudite (tr.)	H.072
$Na_2MnFe^{2+}Fe^{3+}(PO_4)_3$	400	1	NNO	6	Alluaudite	H.084
	400	1	CT	3	Alluaudite	H.119
	400	1	HI	3	Marićite + alluaudite + ?	H.127
	500	1	NNO	12	Alluaudite + marićite	H.093
	500	1	HM	3	Alluaudite	H.124
	500	1	CT	3	Alluaudite	H.120
	500	1	HI	3	Marićite + $(Fe^{2+},Mn)_2P_2O_7$ + ? (tr.)	H.128
	500	2	NNO	7	Alluaudite + marićite (tr.)	H.102
	500	3	NNO	12	Alluaudite + marićite	H.095
	600	1	NNO	6	Alluaudite + marićite	H.078
	600	1	HM	4	Alluaudite	H.106
	600	1	CT	4	Alluaudite + hematite	H.111
	600	2	NNO	7	Alluaudite + marićite	H.103
	600	3	NNO	12	Alluaudite + marićite	H.096
	700	1	NNO	12	Alluaudite + marićite	H.094
	700	1	HM	4	Alluaudite	H.201
	700	1	CT	3	Alluaudite + hematite	H.121
	700	2	NNO	7	Alluaudite + marićite	H.104
	700	3	NNO	12	Alluaudite + marićite	H.097
	800	1	NNO	6	X-phase + marićite + alluaudite	H.073
	800	1	–	3	X-phase + alluaudite + marićite	H.126[a]
$Na_2Mn_{0,5}Fe^{2+}{}_{1,5}Fe^{3+}(PO_4)_3$	400	1	NNO	6	Alluaudite	H.085
	500	1	NNO	7	Alluaudite	H.138
	600	1	NNO	6	Alluaudite + marićite	H.079
	600	1	HM	4	Alluaudite	H.107
	600	1	CT	4	Alluaudite + hematite + ?	H.112
	700	1	NNO	7	Alluaudite + marićite	H.100
	700	1	HM	4	Alluaudite	H.202
	800	1	NNO	6	Marićite + X-phase + alluaudite	H.074
$Na_2Fe^{2+}{}_2Fe^{3+}(PO_4)_3$	400	1	NNO	6	Alluaudite	H.086
	400	1	HM	3	Alluaudite	H.212
	500	1	NNO	7	Alluaudite	H.139
	600	1	NNO	6	Alluaudite + marićite	H.080
	600	1	HM	4	Alluaudite	H.108
	600	1	CT	4	Alluaudite + hematite + ?	H.113
	700	1	NNO	7	Alluaudite + marićite	H.101
	700	1	HM	4	Alluaudite	H.203
	800	1	NNO	6	Marićite + X-phase + alluaudite + ? (tr.)	H.075

[a] Buffer used up; results not used for systematic phase relations

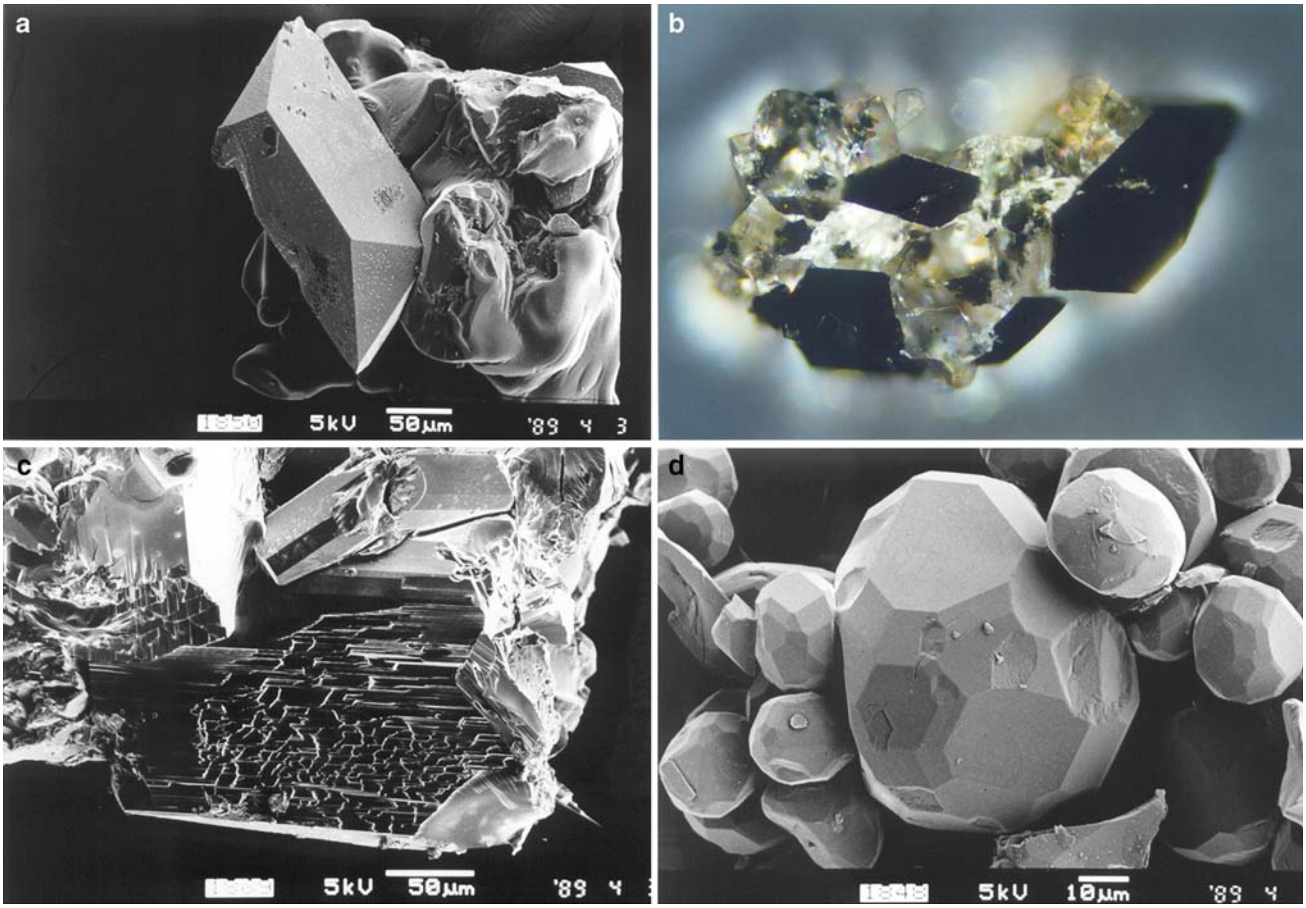

Fig. 3 **a** Alluaudite crystal which shows the forms {110} and {011} on marićite. Sample H.114, scanning electron microscope, secondary electron image. **b** Colorless grain of marićite with an irregular shape, including large black euhedral crystals of alluaudite. Sample H.115, reflected light microscope, crossed polars. The long edge of the photograph is approximately 800 µm. **c** Prismatic crystal of ‘‘X-phase’’, with cleavage planes parallel to the elongation. Sample H.126, scanning electron microscope, secondary electron image. **d** Crystals of fillowite, showing numerous faces. Sample H.114, scanning electron microscope, secondary electron image

calculated unit-cell parameters of synthetic marićite-type compounds are given in Table 3. The electron-microprobe analyses (Table 5) show that a complete solid solution exists between $NaFe^{2+}(PO_4)$ and $NaMn(PO_4)$. The $NaMn(PO_4)$ end-member is not included in the present study, but it has been obtained hydrothermally at 600°C and 1 kbar (Hatert 2002).

In order to estimate the $Fe_{total}/(Fe_{total} + Mn)$ ratio of marićite-type compounds, correlations have been established between this ratio and the unit-cell parameters (Fig. 5). The $Fe_{total}/(Fe_{total} + Mn)$ ratios of marićites synthesized at low temperatures, estimated with the correlations given in Fig. 5, are presented in Table 4.

‘‘X-phase’’

In the experiments performed at 800°C, the powder X-ray diffraction patterns show the presence of a phosphate similar to the one already obtained by solid-state reaction during the investigation of the Na–Mn–Fe^{3+} (+ PO_4) system (Hatert 2002). This compound, named ‘‘X-phase’’, occurs as large crystals reaching 1 mm in length, elongated and showing a good cleavage parallel to their elongation (Fig. 3c). The crystals exhibit a brownish color similar to that of fillowite-type phosphates. The electron-microprobe analyses (Table 6) show a $(Na + Mn + Fe_{total})/P$ ratio very close to 7/4, and chemical compositions similar to those of fillowites, with but with a significant enrichment in Na and Fe_{total}. It is also important to note the low totals of the microprobe analyses (Table 6), which could be related to the presence of H_2O or OH^- groups in the structure.

Several datasets were collected on a Bruker P4 4-circle diffractometer, in order to solve the crystal structure of ‘‘X-phase’’, but the presence of satellite reflections indicates that this crystal structure is probably modulated. For this reason, the refinements were very poor, with an R_1 factor higher than 12%. The measured unit-cell parameters are a = 25.892(4), b = 14.792(5), and c = 10.364(2) Å, for space group *Pnma* or *Pna*2$_1$. Complementary measurements on a diffractometer equipped with a CCD detector are now in progress, in order to solve this crystal structure.

The unit-cell parameters measured on samples of "X-phase" synthesized in this study are given in Table 3, and the correlations between the $Fe_{total}/(Fe_{total} + Mn)$ ratio and the unit-cell parameters are shown in Fig. 6. The very large variation of the a parameter, when compared to b and c (Fig. 6), indicates that the $Mn^{2+} \rightarrow Fe^{2+}$ substitution probably takes place on one or several crystallographic sites aligned along the a axis.

Fillowite-type phosphates

Fillowite, $Na_2Ca(Mn,Fe^{2+})_7(PO_4)_6$, is a phosphate mineral occurring in numerous rare-element granitic pegmatites (Fransolet et al. 1998). Experiments performed in this study, starting from the composition $Na_2Mn_2Fe^{3+}(PO_4)_3$, have shown the presence of fillowite-type phosphates associated with alluaudite, marićite, or "X-phase", between 600 and 800°C and under the oxygen fugacity controlled by the NNO buffer (Table 1). Isometric fillowite crystals, brownish in color, can reach 500 μm in diameter and exhibit a complex morphology characterized by the presence of numerous faces (Fig. 3d).

The electron-microprobe analysis given in Table 6, as well as those presented by Hatert (2004b), indicates chemical compositions localized in the Mn-rich part of the Na–Mn–Fe_{total} ternary diagram, in good agreement with the data for pegmatitic fillowites from Central Africa (Fransolet et al. 1998). The presence of Fe^{3+} in synthetic fillowites has been noted by Hatert (2004b), who suggests the substitution mechanism $Mn^{2+} + 2Fe^{2+} \rightarrow \square + 2Fe^{3+}$, similar to that occurring in alluaudites. Fransolet et al. (1998) reported up to 2.76 wt% Fe_2O_3 in natural fillowites.

The crystal structure of a synthetic fillowite crystal with composition $Na(Na,Mn)_7Mn_{22}(PO_4)_{18}\cdot 0.5H_2O$ has been solved by Keller et al. (2006) in the $R\bar{3}$ space group. The unit-cell parameters are a = 15.2741(9) and c = 43.335(3) Å, and the refined crystal structure is very similar to that described by Araki and Moore (1981) for natural fillowite. However, a supplementary oxygen position O(25) in synthetic fillowite has been attributed to the presence of H_2O in the structure, and confirmed by infrared spectroscopy (Keller et al. 2006).

Table 2 Electron-microprobe analyses of alluaudite-type compounds, hydrothermally synthesized from the $Na_2(Mn_{2-2x}Fe_{1+2x})(PO_4)_3$ starting compositions

	H.073	H.074	H.075	H.076	H.094	H.095	H.096	H.097	H.099	H.100	H.101	H.103	H.104	H.121
	(8)	(4)	(4)	(1)	(5)	(7)[a]	(6)[a]	(6)[a]	(6)	(9)	(6)	(6)[a]	(7)[a]	(7)[a]
x	0.50	0.75	1.00	0.00	0.50	0.50	0.50	0.50	0.25	0.75	1.00	0.50	0.50	0.50
P_2O_5	41.18	41.18	41.36	41.35	40.78	43.41	43.37	43.02	40.94	41.58	42.52	43.52	43.20	44.27
Fe_2O_3[b]	8.20	10.13	11.15	7.18	8.17	19.29	16.15	17.07	7.08	13.30	14.16	19.81	19.13	27.51
Mn_2O_3[b]	0.00	0.00	0.00	0.00	0.00	0.00	0.00	0.00	0.00	0.00	0.00	0.00	0.00	3.09
FeO[b]	22.43	28.71	36.03	11.73	22.36	12.48	15.31	15.27	18.00	24.15	31.63	10.97	12.84	0.00
MnO	17.04	7.44	0.00	28.40	15.06	14.81	15.86	14.68	21.44	7.71	0.00	15.81	14.43	11.65
Na_2O	10.17	10.28	10.07	10.88	11.45	10.70	10.92	10.48	11.13	11.41	11.90	10.62	10.63	12.15
Total	99.02	97.74	98.61	99.54	97.82	100.69	101.61	100.52	98.59	98.15	100.21	100.73	100.23	98.67
Cation numbers on the basis of 3 P per formula unit														
P	3.000	3.000	3.000	3.000	3.000	3.000	3.000	3.000	3.000	3.000	3.000	3.000	3.000	3.000
Fe^{3+}	0.531	0.656	0.719	0.463	0.534	1.185	0.993	1.058	0.461	0.853	0.888	1.214	1.181	1.657
Mn^{3+}	0.000	0.000	0.000	0.000	0.000	0.000	0.000	0.000	0.000	0.000	0.000	0.000	0.000	0.188
Fe^{2+}	1.614	2.066	2.582	0.841	1.625	0.852	1.046	1.052	1.303	1.721	2.205	0.747	0.881	0.000
Mn^{2+}	1.242	0.542	0.000	2.061	1.109	1.024	1.098	1.024	1.572	0.556	0.000	1.091	1.002	0.790
Na	1.696	1.716	1.672	1.807	1.930	1.693	1.730	1.674	1.868	1.886	1.923	1.677	1.691	1.885
Fe^{3+} (%)	24.8	24.1	21.8	35.5	24.7	58.2	48.7	50.1	26.1	33.1	28.7	61.9	57.3	100.0
$Fe_{total}/(Fe_{total} + Mn)$	0.633	0.834	1.000	0.388	0.661	0.665	0.650	0.673	0.529	0.822	1.000	0.643	0.673	0.629
$\square$	– 0.083	0.020	0.027	– 0.172	– 0.198	0.246	0.133	0.192	– 0.204	– 0.016	– 0.016	0.271	0.245	0.480

The number of point analyses is indicated in parentheses. Analysts: F. Fontan, P. de Parseval, or J. Wautier

[a] Analyses performed in Louvain-la-Neuve by J. Wautier

[b] The FeO and Fe_2O_3 values have been calculated to maintain charge balance. When all iron was on the trivalent state, Mn_2O_3 was also introduced to achieve charge balance

Table 3 Unit-cell parameters of the phosphates hydrothermally synthesized from the $Na_2(Mn_{2-2x}Fe_{1+2x})(PO_4)_3$ starting compositions

Run no.	x	a (Å)	b (Å)	c (Å)	β (°)	Vol. ($Å^3$)
Alluaudites						
H.076	0.00	12.006(2)	12.625(2)	6.506(1)	114.78(1)	895.3(2)
H.077	0.25	11.987(4)	12.595(3)	6.498(2)	114.75(2)	890.9(3)
H.078	0.50	11.942(2)	12.574(1)	6.4944(8)	114.66(1)	886.2(1)
H.079	0.75	11.905(2)	12.550(2)	6.4857(8)	114.59(1)	881.2(1)
H.080	1.00	11.843(3)	12.532(2)	6.482(2)	114.60(2)	874.7(2)
H.081	0.00	11.995(4)	12.616(3)	6.496(2)	114.63(2)	893.5(3)
H.082	0.00	12.024(4)	12.629(6)	6.515(3)	114.58(4)	899.6(5)
H.083	0.25	11.995(3)	12.596(4)	6.495(2)	114.60(3)	892.3(3)
H.084	0.50	11.944(2)	12.560(2)	6.480(1)	114.52(1)	884.4(2)
H.085	0.75	11.894(4)	12.536(3)	6.471(2)	114.49(2)	878.1(3)
H.086	1.00	11.849(2)	12.539(1)	6.4861(9)	114.51(1)	876.8(1)
H.093	0.50	11.941(3)	12.569(3)	6.489(1)	114.55(2)	886.0(3)
H.094	0.50	11.928(2)	12.576(2)	6.498(1)	114.67(2)	885.7(2)
H.099	0.25	11.974(5)	12.582(6)	6.515(2)	114.92(3)	890.1(1)
H.100	0.75	11.901(4)	12.551(3)	6.501(2)	114.79(3)	881.6(3)
H.101	1.00	11.841(4)	12.539(4)	6.483(2)	114.62(3)	875.1(3)
H.110	0.25	12.004(2)	12.583(2)	6.4823(9)	114.36(1)	891.9(2)
H.111	0.50	12.017(3)	12.532(3)	6.456(1)	114.26(2)	886.4(3)
H.112	0.75	12.084(2)	12.471(2)	6.434(2)	114.31(1)	883.6(2)
H.113	1.00	12.112(2)	12.448(2)	6.421(2)	114.50(2)	880.9(2)
H.136	0.00	11.996(4)	12.635(4)	6.522(2)	114.82(3)	897.2(3)
H.137	0.25	11.962(2)	12.606(2)	6.505(1)	114.62(2)	891.6(2)
Marićites						
H.072	0.25	6.878(3)	9.004(5)	5.071(2)	90.00	314.0(4)
H.073	0.50	6.869(3)	9.013(5)	5.055(2)	90.00	312.9(4)
H.074	0.75	6.864(2)	9.000(3)	5.054(1)	90.00	312.2(2)
H.075	1.00	6.862(4)	8.976(6)	5.040(2)	90.00	310.4(5)
H.076	0.00	6.891(2)	9.065(4)	5.097(1)	90.00	318.4(3)
H.077	0.25	6.889(5)	9.051(8)	5.084(2)	90.00	317.0(6)
H.078	0.50	6.867(4)	9.022(6)	5.068(2)	90.00	314.0(5)
H.079	0.75	6.877(4)	8.984(7)	5.047(2)	90.00	311.9(6)
H.080	1.00	6.882(5)	8.944(9)	5.085(3)	90.00	313.0(7)
H.081	0.00	6.895(4)	9.073(7)	5.100(2)	90.00	319.1(5)
H.082	0.00	6.89(1)	9.10(2)	5.115(8)	90.00	321(2)
H.093	0.50	6.915(7)	9.01(1)	5.050(4)	90.00	315(1)
H.094	0.50	6.871(3)	9.013(6)	5.066(2)	90.00	313.7(5)
H.099	0.25	6.889(4)	9.035(7)	5.100(2)	90.00	317.4(5)
H.100	0.75	6.858(2)	8.997(3)	5.049(1)	90.00	311.6(3)
H.101	1.00	6.864(4)	8.986(6)	5.040(2)	90.00	310.8(5)
H.136	0.00	6.894(4)	9.070(7)	5.111(2)	90.00	319.6(6)
H.137	0.25	6.926(6)	9.02(1)	5.077(3)	90.00	317.2(9)
"X-phase"						
H.071	0.00	26.076(7)	14.857(2)	10.371(1)	90.00	4,018(2)
H.072	0.25	25.969(8)	14.819(3)	10.358(1)	90.00	3,986(3)
H.073	0.50	25.894(9)	14.803(3)	10.347(2)	90.00	3,966(3)
H.074	0.75	25.79(1)	14.808(4)	10.306(2)	90.00	3,936(4)
H.075	1.00	25.69(1)	14.784(5)	10.286(2)	90.00	3,906(4)
H.098	0.00	26.06(1)	14.854(4)	10.376(2)	90.00	4,016(3)

Hematite

Hematite has been observed in association with alluaudite at 600 and 700°C, under the very high oxygen fugacity fixed by the CT buffer (Table 1). The electron-microprobe analysis of the tabular crystals obtained in run no. H.121 shows a content of 0.40 wt% MnO (Table 6).

$(Fe,Mn)_2P_2O_7$

Starting from the composition $Na_2MnFe^{2+}Fe^{3+}(PO_4)_3$, the experiment performed at 500°C, under the very low oxygen fugacity fixed by the MI buffer (run no. H.128, Table 1), produces large colorless euhedral crystals of $(Fe^{2+},Mn)_2P_2O_7$ (Stefanidis and Nord 1984), associated with marićite. The electron-microprobe analysis

Fig. 4 Variation of the unit-cell parameters of alluaudite-type phosphates versus $Fe_{total}/(Fe_{total} + Mn)$. Linear regressions correspond to the equations: $a = -0.2629X + 12.118$ ($R^2 = 0.973$), $b = -0.1419X + 12.667$ ($R^2 = 0.923$), $c = -0.0482X + 6.5247$ ($R^2 = 0.558$), $\beta = -0.1454X + 114.77$ ($R^2 = 0.079$), $V = -34.948X + 909.15$ ($R^2 = 0.976$). These diagrams also include data given by Hatert (2002)

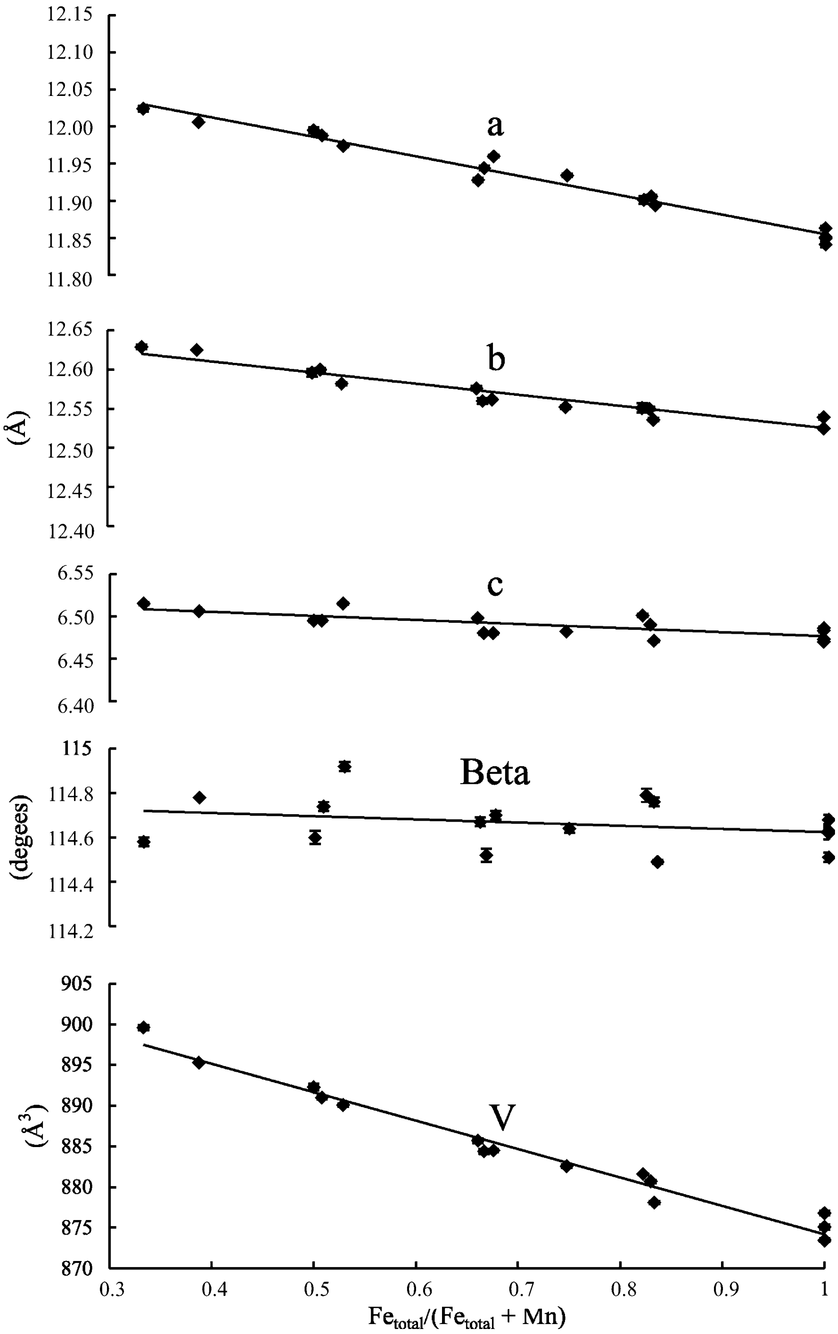

(Table 6) confirms the absence of Na and indicates a $Fe_{total}/(Fe_{total} + Mn)$ ratio close to 0.5.

Phase relations

The synthesis experiments performed by Hatert (2004b), as well as those reported in the present paper (Table 1), clearly demonstrate that alluaudite-type phosphates are very stable in the Na–Mn–Fe^{2+}–Fe^{3+} (+ PO_4) quaternary system. This behavior is probably related to the extreme flexibility of the alluaudite structure, which is able to incorporate numerous exotic cations (Hatert 2004a). The best way to achieve a good knowledge of the stability of natural alluaudites would be to investigate the phase relations in the whole Na–Mn–Fe^{2+}–Fe^{3+} (+ PO_4) quaternary diagram. However, in order to simplify this very complex problem, we decided first to investigate the stability of the $Na_2(Mn_{2-2-x}Fe_{1+2x})(PO_4)_3$ system, which represents the idealized compositions of natural primary alluaudites. The following results are based on

Table 4 $Fe_{total}/(Fe_{total} + Mn)$ ratios of alluaudite- and marićite-type phosphates, calculated from their unit-cell parameters

Alluaudites		Marićites	
Run no.	$Fe_{total}/(Fe_{total} + Mn)$	Run no.	$Fe_{total}/(Fe_{total} + Mn)$
H.077	0.51(1)	H.077	0.34(8)
H.078	0.661(8)	H.078	0.7(1)
H.079	0.81(1)	H.079	0.8(2)
H.080	0.99(5)	–	–
H.081	0.43(6)	H.081	0.18(6)
–	–	H.082	0.0(2)
H.093	0.68(1)	H.093	0.7(2)
H.110	0.51(8)	–	–
H.111	0.7(3)	–	–
H.112	0.7(6)	–	–
H.113	0.8(8)	–	–
H.136	0.3(1)	H.136	0.11(4)
H.137	0.51(8)	H.137	0.5(1)

These values are averages of the $Fe_{total}/(Fe_{total} + Mn)$ ratios calculated with the equations of Figs. 4 and 5, starting from *a*, *b*, and *V* (alluaudites) or from *a*, *b*, *c* and *V* (marićites)

synthesis experiments, but a few reversal runs indicate that the observed phosphate associations are close to the equilibrium state.

The influence of temperature

Results between 400 and 800°C (NNO, P = 1 kbar)

In order to understand the temperature stability of the $Na_2(Mn_{2-2x}Fe_{1+2x})(PO_4)_3$ system, we performed hydrothermal experiments at 400, 500, 600, 700, and 800°C, under a pressure of 1 kbar and an oxygen fugacity controlled by the NNO buffer, which seem to be appropriate for the formation of alluaudites in granitic pegmatites. The results of these experiments (Table 1) are presented in Fig. 7, which clearly shows that single-phase alluaudites crystallize at 400 and 500°C, whereas the association alluaudite + marićite appears between 500 and 700°C. Consequently, the

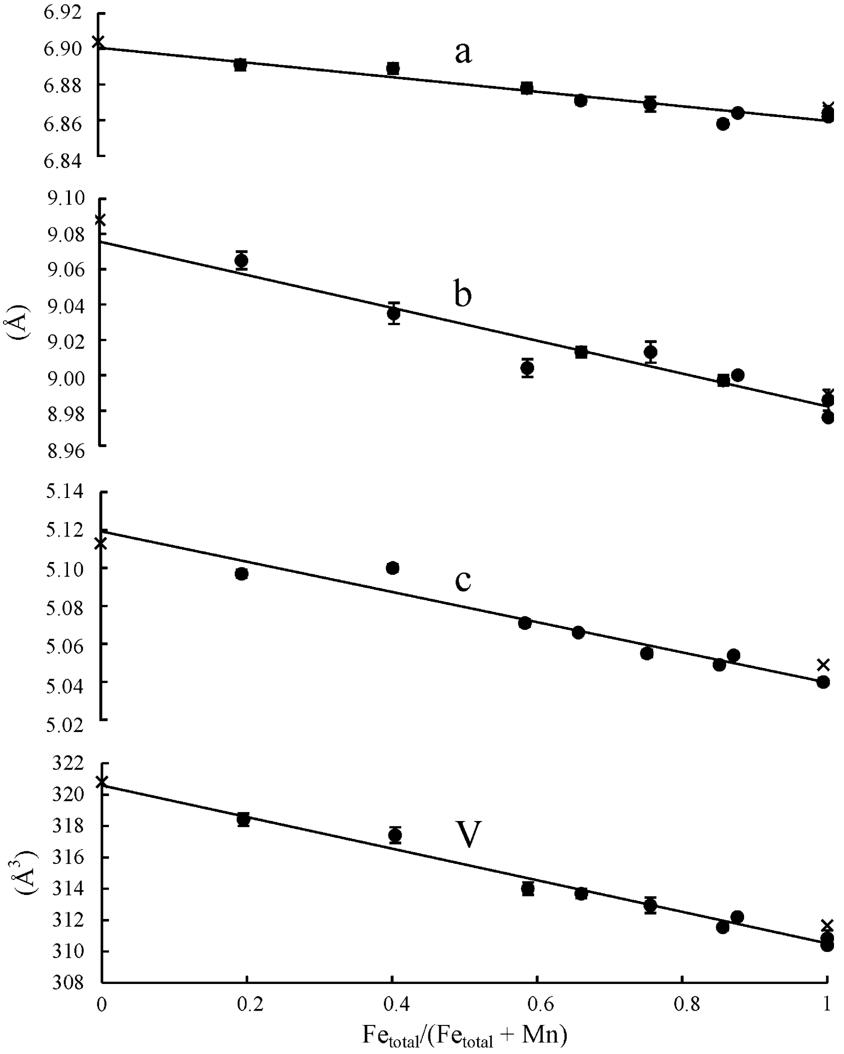

Fig. 5 Variation of the unit-cell parameters of marićite-type phosphates versus $Fe_{total}/(Fe_{total} + Mn)$. Linear regressions correspond to the equations: $a = -0.041X + 6.9007$ ($R^2 = 0.895$), $b = -0.0935X + 9.0757$ ($R^2 = 0.911$), $c = -0.0793X + 5.1193$ ($R^2 = 0.936$), $V = -10.066X + 320.58$ ($R^2 = 0.970$). The *crosses* represent the data for synthetic $NaFe^{2+}(PO_4)$ (Bridson et al. 1998) and synthetic $NaMn(PO_4)$ (Moring and Kostiner 1986)

Table 5 Electron-microprobe analyses of marićite-type compounds, hydrothermally synthesized from the $Na_2(Mn_{2-2-x}Fe_{1+2x})(PO_4)_3$ starting compositions

	H.072	H.073	H.074	H.075	H.076	H.094	H.095	H.096	H.097	H.098	H.099	H.100	H.101	H.103	H.104	H.128
	(12)	(6)	(6)	(4)	(6)	(5)	(6)[a]	(6)[a]	(6)[a]	(2)	(5)	(5)	(3)	(6)[a]	(5)[a]	(6)[a]
x	0.25	0.50	0.75	1.00	0.00	0.50	0.50	0.50	0.50	0.00	0.25	0.75	1.00	0.50	0.50	0.50
P_2O_5	39.77	39.63	39.81	39.61	39.33	39.47	41.74	41.70	42.01	38.91	39.00	40.00	40.15	41.90	41.92	41.54
FeO	24.72	31.74	36.87	41.93	8.39	27.60	32.83	28.05	27.20	14.97	17.10	34.75	40.57	29.90	27.49	31.64
MnO	17.18	10.12	5.14	0.00	34.23	14.01	8.97	13.35	14.18	27.19	24.91	5.75	0.00	11.74	13.80	10.24
Na_2O	17.59	17.45	17.53	17.44	17.27	17.51	17.20	17.35	17.11	17.09	17.45	17.66	17.99	17.25	17.11	16.74
Total	99.26	98.94	99.35	98.98	99.22	98.59	100.74	100.46	100.51	98.16	98.46	98.16	98.71	100.79	100.32	100.16
Cation numbers on the basis of 4 O per formula unit, assuming all iron as Fe^{2+}																
P	0.987	0.988	0.988	0.988	0.979	0.987	1.009	1.012	1.014	0.980	0.979	0.998	0.997	1.011	1.014	1.010
Fe^{2+}	0.606	0.781	0.904	1.032	0.207	0.682	0.784	0.673	0.649	0.372	0.424	0.856	0.995	0.713	0.657	0.760
Mn	0.426	0.252	0.128	0.000	0.853	0.350	0.217	0.324	0.343	0.685	0.626	0.144	0.000	0.283	0.334	0.250
Na	1.000	0.996	0.996	0.996	0.985	1.003	0.953	0.965	0.946	0.986	1.004	1.009	1.023	0.953	0.948	0.932
$Fe_{total}/(Fe_{total}+Mn)$	0.587	0.756	0.876	1.000	0.195	0.661	0.783	0.675	0.654	0.352	0.404	0.856	1.000	0.716	0.663	0.753

The number of point analyses is indicated in parentheses. Analysts: F. Fontan, P. de Parseval, or J. Wautier

[a] Analyses performed in Louvain-la-Neuve by J. Wautier

upper stability limits of ferrohagendorfite, $Na_2Fe^{2+}{}_2Fe^{3+}(PO_4)_3$ ($x = 1.00$), of hagendorfite, $Na_2MnFe^{2+}Fe^{3+}(PO_4)_3$ ($x = 0.50$), and of varulite, $Na_2Mn_2Fe^{3+}(PO_4)_3$ ($x = 0.00$), correspond to 550–600, 450–500, and 350–400°C, respectively. These data indicate that Mn-rich alluaudites crystallize at lower temperatures than Fe-rich alluaudites.

The electron-microprobe analyses (Tables 2, 5) show that alluaudites are depleted in Na when they are associated with marićites, and that the $Fe_{total}/(Fe_{total} + Mn)$ ratios of these phosphates are similar. Taking these observations into account, it is possible to write the reactions which could explain the crystallization of marićite:

$$Na_2MnFe^{2+}Fe^{3+}(PO_4)_3 \rightarrow 0.23\,Na(Fe^{2+}_{0.67}Mn_{0.33})(PO_4) + 0.92\,Na_{1.93}Mn_{1.00}Fe^{2+}_{0.93}Fe^{3+}_{1.07}(PO_4)_3,\text{ and}$$

Table 6 Electron-microprobe analyses of miscellaneous compounds, hydrothermally synthesized from the $Na_2(Mn_{2-2x}Fe_{1+2x})(PO_4)_3$ starting compositions

	"X-phase"						Fillowite	$(Fe,Mn)_2P_2O_7$	Hematite
	H.071	H.072	H.073	H.074	H.075	H.098	H.076	H.128	H.121
	(12)	(17)	(15)	(9)	(14)	(7)	(5)	(6)[a]	(2)[a]
x	0.00	0.25	0.50	0.75	1.00	0.00	0.00	0.50	0.50
P_2O_5	39.76	39.89	39.91	39.19	39.94	39.98	39.02	50.70	0.00
$Fe_2O_3^{b}$	0.00	0.97	0.82	0.00	1.84	4.63	0.00	0.00	97.55
FeO^{b}	18.32	23.29	31.37	40.37	47.32	11.55	7.78	27.35	0.00
MnO	32.30	26.10	17.45	9.16	0.00	34.49	43.39	22.90	0.40
Na_2O	8.20	8.24	9.00	9.47	9.33	6.88	8.25	0.00	0.00
Total	98.58	98.49	98.55	98.19	98.43	97.53	98.44	100.95	97.95
Cation numbers									
P	4.000	4.000	4.000	4.000	4.000	4.000	6.000	2.009	0.000
Fe^{3+}	0.000	0.087	0.073	0.000	0.164	0.412	0.000	0.000	1.991
Fe^{2+}	1.820	2.307	3.107	4.071	4.681	1.141	1.182	1.071	0.000
Mn	3.251	2.619	1.749	0.936	0.000	3.452	6.674	0.908	0.009
Na	1.888	1.892	2.067	2.213	2.141	1.577	2.906	0.000	0.000
$\Sigma_{cat.}$	6.959	6.905	6.996	7.220	6.986	6.582	10.762	1.979	2.000
Fe^{3+} (%)	0.0	3.6	2.3	0.0	3.4	26.5	0.0	0.0	100.0
$Fe_{total}/(Fe_{total} + Mn)$	0.359	0.478	0.645	0.813	1.000	0.310	0.150	0.541	0.996

The number of point analyses is indicated in parentheses, and the cation numbers have been calculated on the basis of 4 P ("X-phase"), 6 P (fillowite), 7 O ($(Fe,Mn)_2P_2O_7$), and two atoms (hematite) per formula unit. Analysts: F. Fontan, P. de Parseval, or J. Wautier

[a] Analyses performed in Louvain-la-Neuve by J. Wautier

[b] For fillowite and "X-phase", FeO and Fe_2O_3 values have been calculated to maintain charge balance, whereas all iron was expressed as FeO in $(Fe,Mn)_2P_2O_7$ and as Fe_2O_3 in hematite

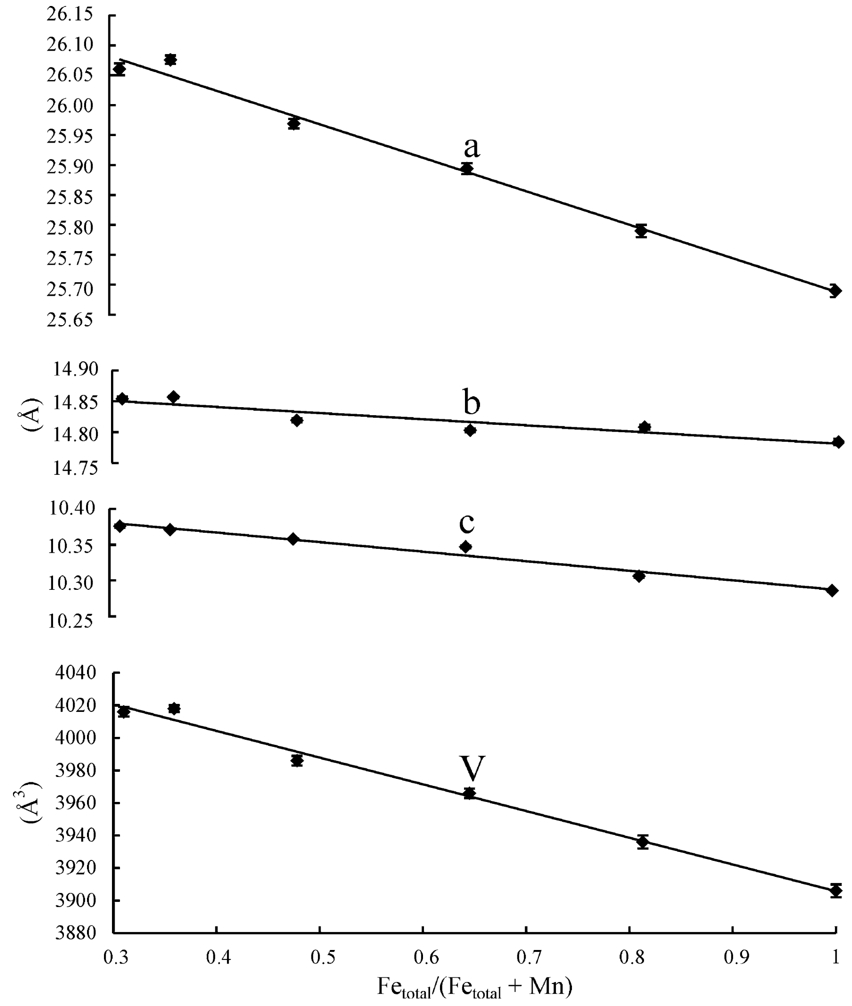

Fig. 6 Variation of the unit-cell parameters of "X-phase" versus $Fe_{total}/(Fe_{total} + Mn)$. Linear regressions correspond to the equations: $a = -0.5625X + 26.251$ ($R^2 = 0.990$), $b = -0.0998X + 14.881$ ($R^2 = 0.854$), $c = -0.1335X + 10.421$ ($R^2 = 0.969$), $V = -164.32X + 4070.1$ ($R^2 = 0.991$)

$$Na_2Fe_2^{2+}Fe^{3+}(PO_4)_3 \rightarrow 0.23\,NaFe^{2+}(PO_4) + 0.92\,Na_{1.93}Fe_{1.93}^{2+}Fe_{1.07}^{3+}(PO_4)_3.$$

At 800°C, the formation of "X-phase" has been reported, in addition to alluaudite and marićite (Fig. 7). It must be pointed out that "X-phase" is observed for variable $Fe_{total}/(Fe_{total} + Mn)$ ratios. Moreover, fillowite is also detected in the Mn-rich part of the diagram.

Compositional variations with temperature

Using the electron-microprobe analyses of the synthetic phosphates (Tables 2, 5, 6), we established the phase relations in the central part of the ternary Na–Mn–Fe_{total} (+ PO_4) diagram (Fig. 8). Some marićite-type crystals synthesized at low temperatures were too small to allow reliable microprobe analysis, and, for this reason, they were positioned on the phase diagrams by using the $Fe_{total}/(Fe_{total} + Mn)$ ratios calculated from their unit-cell parameters (Table 4). In some low-temperature runs (H.077, H.078, H.079, H.080, H.082, H.093, H.136, H.137), the chemical composition of alluaudites had also to be estimated from the $Fe_{total}/(Fe_{total} + Mn)$ ratio (Fig. 4).

The phase diagrams of Fig. 8 clearly show that the field of alluaudites shifts towards Na-poor compositions, when the temperature increases. This behavior is related to the crystallization of marićite, which is Na richer than alluaudite. As shown in Fig. 9, on which the results of electron-microprobe analyses are reported, this Na decrease does not affect the $Fe_{total}/(Fe_{total} + Mn)$ ratio of alluaudites, which remains approximately constant. The Na content of alluaudites evolves from 2 Na pfu at 400°C, to ca. 1.90 and 1.70 Na pfu at 700 and 800°C, respectively (Fig. 9). The alluaudite-type compound $Na_2Mn_2Fe^{3+}(PO_4)_3$, however, shows a different behavior with ca. 1.8 Na pfu at 600°C (Fig. 9). A careful examination of the electron-microprobe analyses performed at 800°C (Table 2) indicates that the Na decrease in alluaudites is compensated by

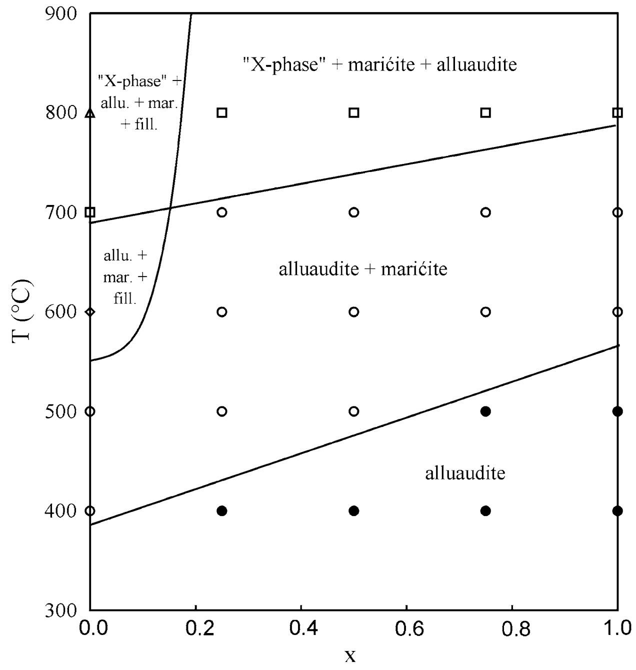

Fig. 7 The phase relations for the $Na_2(Mn_{2-2x}Fe_{1+2x})(PO_4)_3$ system (P = 1 kbar, $f(O_2)$ = NNO). *Closed circles*, alluaudite; *open circles*, alluaudite + marićite; *open diamonds*, alluaudite + marićite + fillowite; *open squares*, "X-phase" + marićite + alluaudite; *open triangle*, "X-phase" + alluaudite + marićite + fillowite

an increase of the Mn content, coupled with a reduction of iron, according to the substitution mechanism: $Na^+ + Fe^{3+} \rightarrow Mn^{2+} + Fe^{2+}$.

As shown in Fig. 8, fillowite crystallizes at 600°C in the Mn-rich part of the Na–Mn–Fe (+ PO_4) diagram, whereas "X-phase" appears at 700 and 800°C. As already observed for alluaudites, Mn-rich "X-phase" crystallizes at a lower temperature than its Fe-rich equivalents (Fig. 8). Note that the overlap between the two stability fields of alluaudite and "X-phase", observed at 800°C (Fig. 8), is due to graphical representation, which corresponds to a projection on one face of the quaternary $Na–Mn–Fe^{2+}–Fe^{3+}$ (+ PO_4) diagram. In fact, alluaudites not only exhibit a significant Na enrichment compared to "X-phase", but also show very different $Fe^{3+}/(Fe^{3+} + Fe^{2+})$ ratios (Tables 2, 6).

The influence of oxygen fugacity

Results between NNO and CT (600°C, P = 1 kbar)

Several runs were performed at 600°C/1 kbar, starting from the compositions $Na_2(Mn_{2-2x}Fe_{1+2x})(PO_4)_3$, under an oxygen fugacity controlled by the NNO, HM, and CT buffers. The results of these experiments are shown in Fig. 10. Under the low oxygen fugacity of the NNO buffer, the assemblage alluaudite + marićite is observed, whereas single-phase alluaudite is obtained under the oxygen fugacity of the HM buffer. This behavior is not surprising, because alluaudite contains iron in both valence states, whereas marićite only contains Fe^{2+}. When the very high oxygen fugacity of the CT buffer is reached, hematite crystallizes in association with alluaudite, thus indicating that most of the iron in the system must be in the trivalent state. Because no Na-bearing phosphate has been detected in these runs, the oxidation mechanism of iron into alluaudite could correspond to:

$$Na_2MnFe^{2+}Fe^{3+}(PO_4)_3 \rightarrow Na_2MnFe^{3+}_{5/3}(PO_4)_3 + 1/6Fe_2O_3.$$

Fillowite-type phosphates occur again in the Mn-rich part of the diagram and under a low oxygen fugacity.

Stability of alluaudites in the f(O₂)–T fields

In order to better understand the influence of oxygen fugacity on the stability of primary alluaudites, additional runs were performed starting from the compositions $Na_2(Mn_{2-2x}Fe_{1+2x})(PO_4)_3$ (x = 0.0–1.0), between 400 and 700°C, at 1 kbar, and under an oxygen fugacity controlled by the HM and CT buffers (Fig. 11). When the oxygen fugacity is controlled by the HM buffer (Fig. 11a), the field of single-phase alluaudite extends from 400 to 700°C for x = 0.25–1.00, whereas the alluaudite + marićite association appears above 500°C for x = 0.00. These data indicate that alluaudite-type phosphates are very stable when the oxygen fugacity is close to HM, except for single-phase Mn-rich varulite, $Na_2Mn_2Fe^{3+}(PO_4)_3$, which is confined to a low-temperature field. When the oxygen fugacity is controlled by the CT buffer (Fig. 11b), single-phase alluaudites are restricted to a low-temperature field, whereas the alluaudite + hematite association appears above 600°C, thus indicating a complete oxidation of iron.

Finally, the stability of hagendorfite, $Na_2MnFe^{2+}Fe^{3+}(PO_4)_3$, has been investigated in the $f(O_2)$–T field at 1 kbar (Fig. 12). Some runs, performed under the very low oxygen fugacity of the MI buffer, show the association marićite + $(Fe^{2+},Mn)P_2O_7$, which indicates a complete reduction of Fe^{3+} into Fe^{2+}. At higher oxygen fugacities, the fields of alluaudite + marićite, of single-phase alluaudite, and of alluaudite + hematite, successively appear. The crystallization of "X-phase" is restricted to a high-temperature domain. Because this diagram provides a rather accurate knowledge of the stability of single-phase hagendorfite in the $f(O_2)$–T

Fig. 8 Phase relations in the central part of the Na–Mn–Fe_{total} (+ PO_4) ternary diagram, between 400 and 800°C (P = 1 kbar, $f(O_2)$ = NNO). *Crosses*, marićite; *open circles*, alluaudite; *open triangles*, fillowite; *open squares*, "X-phase"

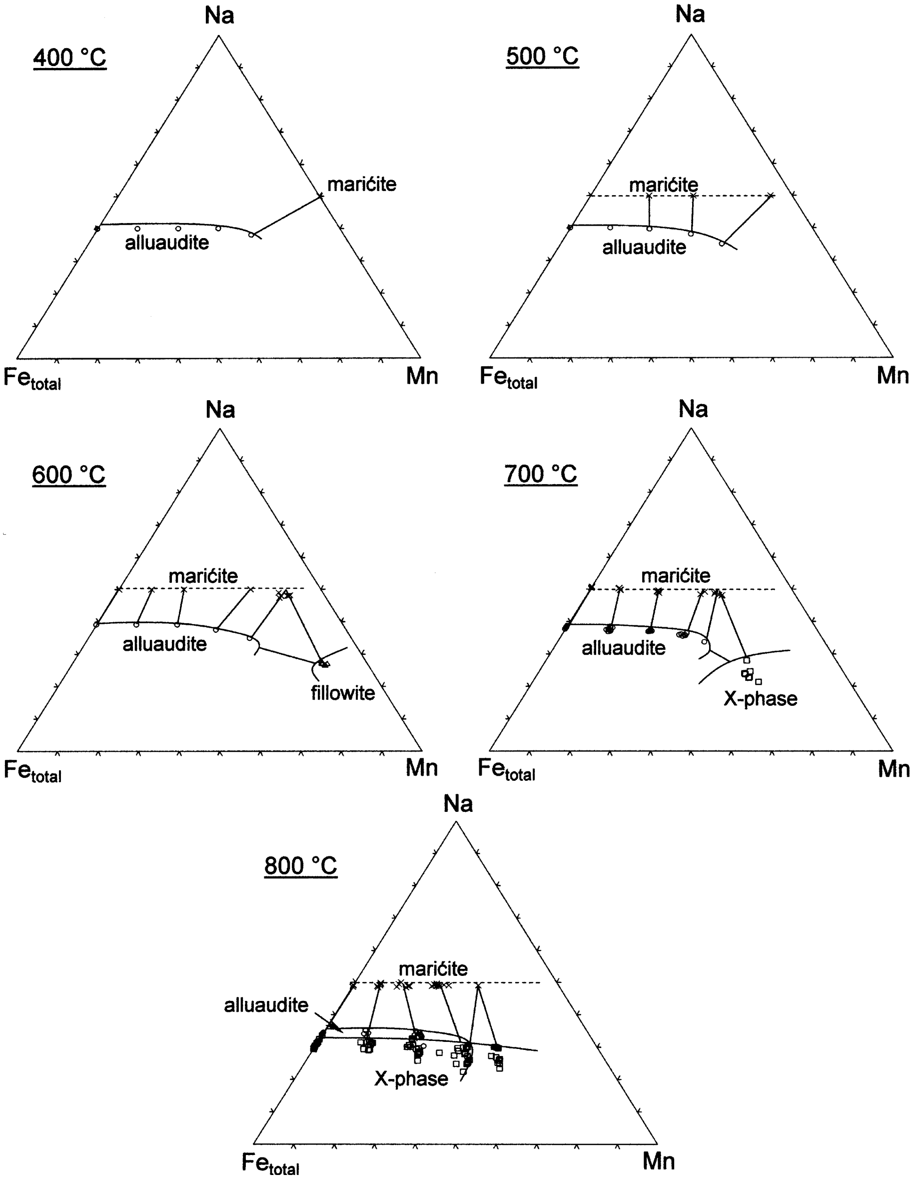

field, it can be used to estimate the oxygen fugacity conditions which prevailed in granitic pegmatites during the crystallization of this phosphate. With the help of independent temperature data, obtained from fluid-inclusion measurements, for example, the temperature can be constrained and the resulting estimate of $f(O_2)$ can be deduced much more accurately.

Discussion

The existence of primary alluaudites in the Buranga pegmatite, Rwanda, was mentioned by Fransolet (1975, 1977) and Héreng (1989), without any replacement texture. In thin section, alluaudite from Buranga shows very large grains with a mosaic texture (Fig. 13a) and sharp contacts with ferrisicklerite, thus confirming the probable primary origin of alluaudite in the pegmatite. Recently, Fransolet et al. (2004) described an unusual association of hagendorfite + heterosite in the Kibingo pegmatite, Rwanda, where primary hagendorfite progressively transforms into secondary oxidized alluaudite (Fig. 13b). As shown by Hatert (2004b), such highly oxidized alluaudites crystallize under a very high oxygen fugacity, because analogous compositions were synthesized in air between 850 and 950°C. The results presented in this paper concern the stability of primary alluaudite in granitic pegmatites, with idealized chemical compositions corresponding to the system $Na_2(Mn_{2-2x}Fe_{1+2x})(PO_4)_3$.

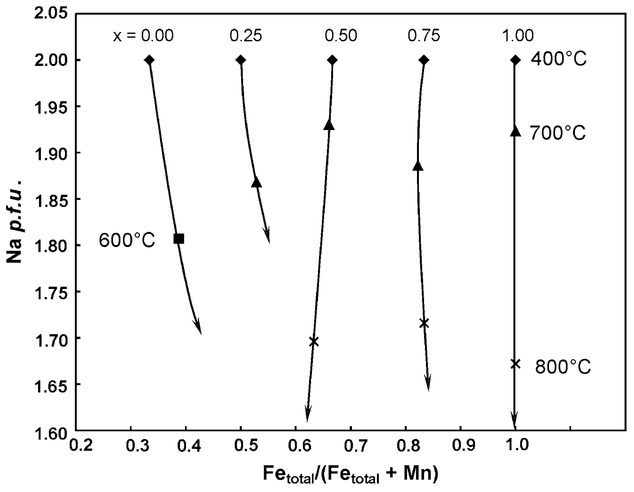

Fig. 9 Variation of the chemical composition of alluaudite between 400 and 800°C (P = 1 kbar, $f(O_2)$ = NNO). *Diamonds*, 400°C; *squares*, 600°C; *triangles*, 700°C; *crosses*, 800°C

Crystallization temperatures of primary alluaudites

The experiments performed in the present study indicate that alluaudites appear to be stable between 400 and 800°C, under oxygen fugacities between those controlled by the NNO and CT buffers. At 1 kbar and under the oxygen fugacity controlled by the NNO buffer, the alluaudites $Na_2Mn_2Fe^{3+}(PO_4)_3$, $Na_2MnFe^{2+}Fe^{3+}(PO_4)_3$, and $Na_2Fe^{2+}{}_2Fe^{3+}(PO_4)_3$ occur below 350–400, 450–500, and 550–600°C, respectively, whereas the association alluaudite + marićite is observed above these temperatures (Fig. 7). The boundary between these two fields should correspond to the upper stability limit of alluaudites in granitic pegmatites, because marićite has never been observed in such geological environments so far. The chemical compositions mentioned above correspond to those of varulite from Varuträsk, Sweden (Quensel 1937, 1940), of hagendorfite from Tsaobismund, Namibia (Fransolet et al. 1986), and of ferrohagendorfite from Angarf-Sud, Morocco (Fransolet et al. 1985), respectively.

The results obtained for alluaudites, for fillowites, and for "X-phase", indicate that Fe-rich phosphates are stable at high temperatures, whereas Mn-rich phosphates are stable at low temperatures only. This observation is in very good agreement with those made on numerous pegmatitic minerals, as for example the phosphates of the triphylite–lithiophilite series, $LiFe^{2+}(PO_4)$–$LiMn(PO_4)$. Fluid inclusion measurements performed by London (1986) and Morgan and London (1987) on minerals from the Tanco pegmatite, Canada, give us an estimate of the crystallization temperatures of several lithiophilite generations (Černý et al. 1996). In the border zone of the pegmatite, the temperature reached 700°C, and $Li(Mn_{0.6}Fe^{2+}_{0.4})(PO_4)$ crystallized, whereas the estimated temperature was only 450°C in the core of the pegmatite, where virtually pure lithiophilite, $LiMn(PO_4)$, was identified. Other well-known isomorphous series of minerals also show a decrease of the $Fe_{total}/(Fe_{total} + Mn)$ ratio during the pegmatite evolution, as for example garnets of the almandine–spessartine series (Baldwin and Von Knorring 1983) or minerals of the columbite–tantalite series (Černý et al. 1985).

Finally, it is important to note that the crystallization of Fe-rich minerals at high temperatures, during the first steps of pegmatite evolution, provokes a progressive decrease of the Fe content of the pegmatite fluid, and a decrease of the $Fe_{total}/(Fe_{total} + Mn)$ ratio, if we consider a closed system. As suggested by Ginzbourg (1960), the Fe/Mn ratio, as well as the Rb/K, Ga/Al, or Hf/Zr ratios, can be used to estimate the degree of pegmatite evolution.

The alluaudite + marićite assemblage

Marićite, $NaFe^{2+}(PO_4)$, has never been reported in granitic pegmatites, whereas it was frequently observed in our experiments. This behavior could be related to the lower temperatures (lower than 400–600°C) and/or to the higher oxygen fugacities of the pegmatites. Another parameter, which has not been taken into account so far, is the existence of other chemical

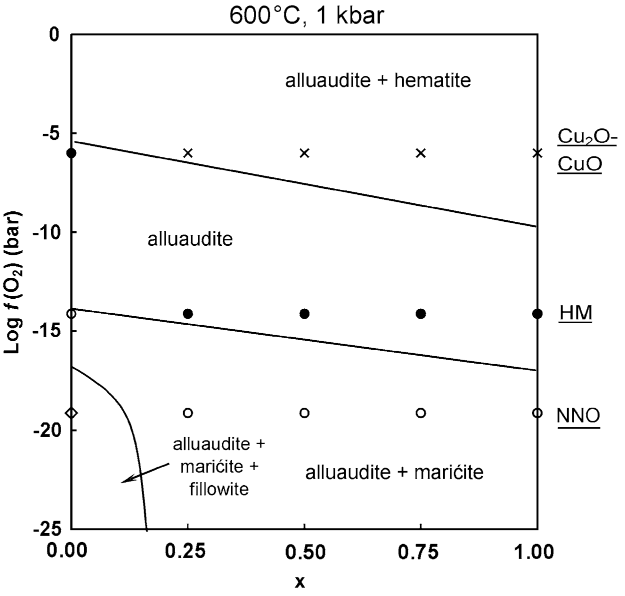

Fig. 10 Phase diagram in the $f(O_2)$–x field, for the $Na_2(Mn_{2-2x}Fe_{1+2x})(PO_4)_3$ system (T = 600°C, P = 1 kbar). *Closed circles*, alluaudite; *open circles*, alluaudite + marićite; *open diamonds*, alluaudite + marićite + fillowite; *crosses*, alluaudite + hematite

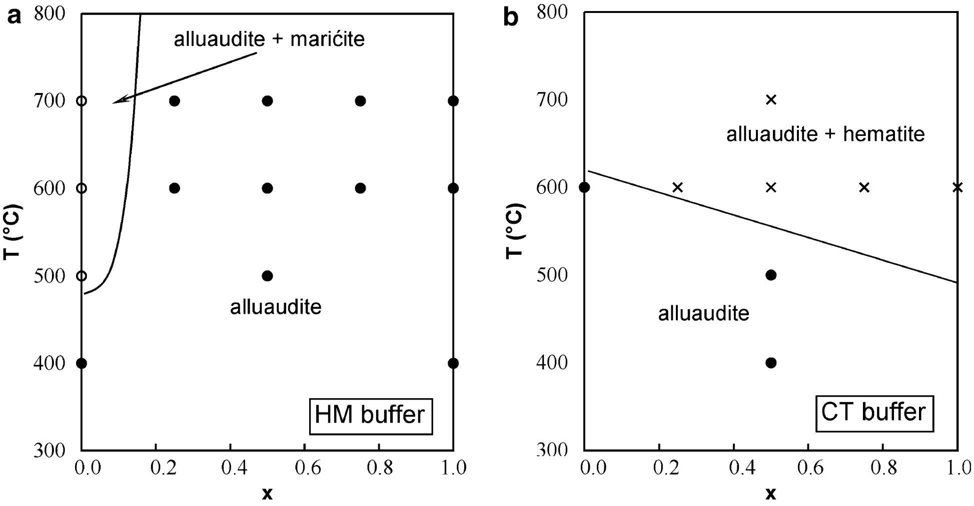

Fig. 11 The phase relations for the $Na_2(Mn_{2-2x}Fe_{1+2x})(PO_4)_3$ system (P = 1 kbar), under an oxygen fugacity controlled by the HM (**a**) or CT (**b**) buffers. *Closed circles*, alluaudite; *open circles*, alluaudite + marićite; *crosses*, alluaudite + hematite

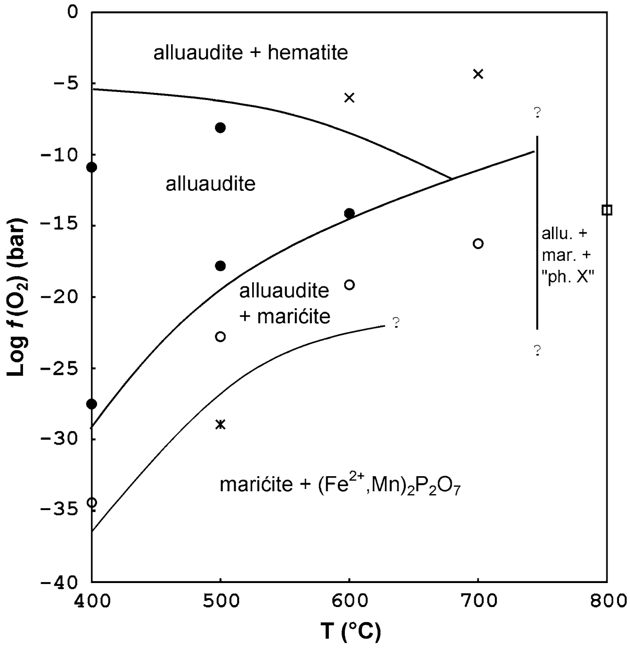

Fig. 12 Phase diagram in the $f(O_2)$–T field for the $Na_2MnFe^{2+}Fe^{3+}(PO_4)_3$ (x = 0.50) alluaudite-type compound (P = 1 kbar). *Closed circles*, alluaudite; *open circles*, alluaudite + marićite; *open squares*, alluaudite + marićite + “X-phase”; *crosses*, alluaudite + hematite; *double crosses*, marićite + $(Fe^{2+},Mn)_2P_2O_7$

elements in the pegmatitic environment. In our closed system, the excess of sodium with regard to iron, manganese, and phosphorous, certainly induces the crystallization of marićite above 500°C. In a more complex natural system where Al and Si are prevailing, the excess of sodium probably leads to the crystallization of Na-bearing aluminosilicates. Albite, for example, occurs in close association with alluaudite and arrojadite in some samples collected by A.-M. Fransolet in the Buranga pegmatite, Rwanda, and tourmaline-group minerals are associated with alluaudite at Varuträsk, Sweden (Quensel 1957) and at Pinilla de Fermoselle, Spain (Roda et al. 2005).

Our data obtained for marićite can also be applied to another geological context, because this mineral occurs in nodules within the metamorphic schists of the Big Fish River, Yukon, Canada (Sturman et al. 1977). Preliminary experiments have shown that at 400 and 700°C (P = 1 kbar, NNO), marićite is associated with alluaudite, thus indicating that the crystallization of single-phase marićite requires an oxygen fugacity lower than that controlled by the NNO buffer. A more detailed petrographic description of the natural marićite samples is also necessary, because Sturman et al. (1977) mention the presence of alluaudite in the nodules from the Big Fish River.

The alluaudite + fillowite assemblage

Alluaudite + fillowite associations have been described by Fransolet et al. (1998) in the pegmatites from Buranga, Rusororo (Rwanda), Nyakishuzoa, and Kabira (Uganda, see Fig. 13c). The absence of reaction textures between these minerals, as well as their mosaic texture (Fig. 13c), indicates that they crystallized together, and constitute a primary alluaudite + fillowite assemblage. This association has been reproduced in our experiments above 600°C (P = 1 kbar, NNO) and in the Mn-rich part of the Na–Mn–Fe^{2+}–Fe^{3+} (+ PO_4) system. This result confirms the observations of Araki and Moore (1981) and Fransolet et al. (1998), who consider fillowite as a primary phosphate. However, it is noteworthy that some chemical compositions reported by Fransolet et al. (1998) for fillowites from Central Africa are significantly richer in Fe, compared to our synthetic Mn-rich fillowite-type phosphates. Fe-rich fillowites are probably stable at a lower oxygen

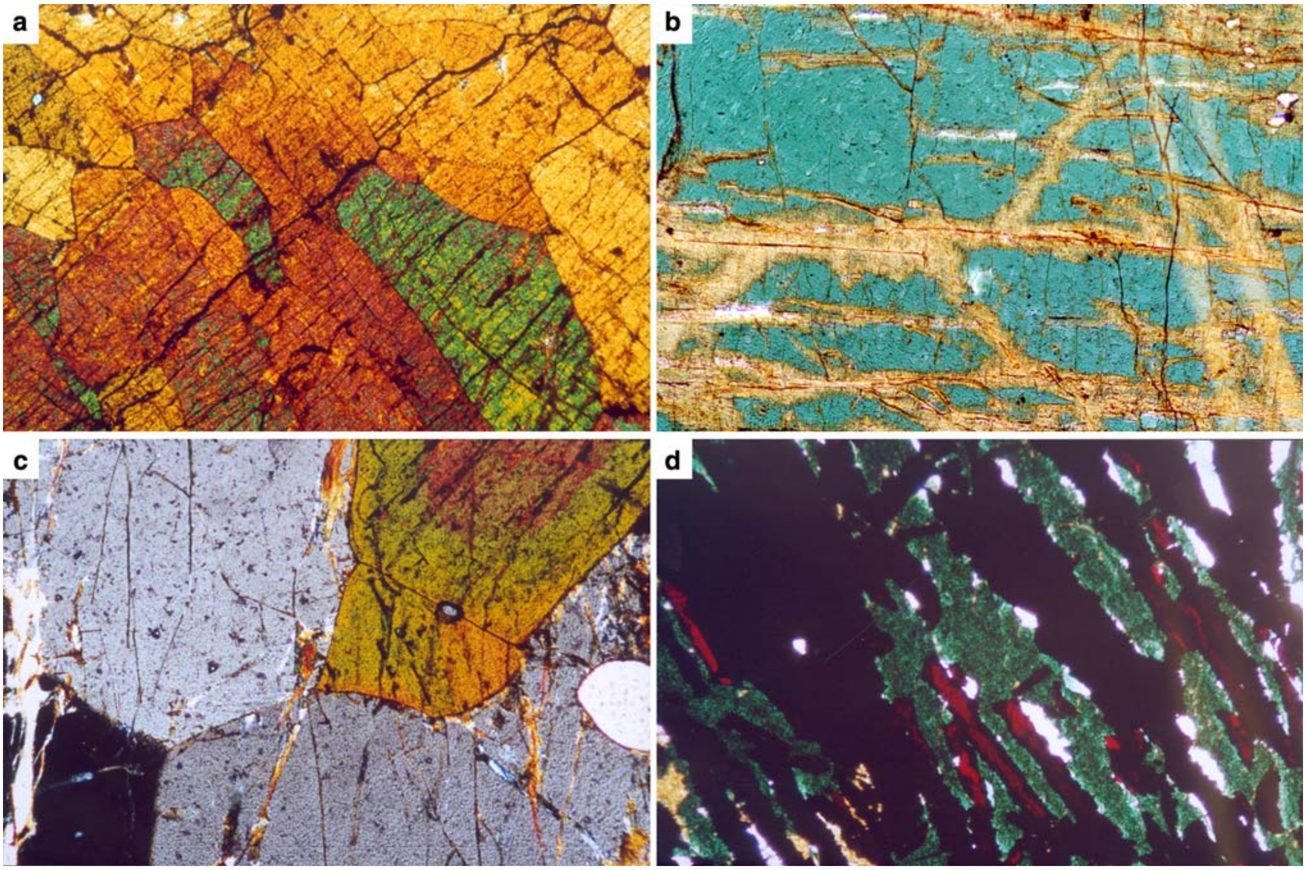

Fig. 13 **a** Large grains of alluaudite from the Buranga pegmatite, in Rwanda, showing a mosaic texture. Transmitted light, crossed polars. The long edge of the photograph is approximately 10 mm. **b** Hagendorfite from the Kibingo pegmatite, Rwanda (*bluish*), which is oxidized along fractures to secondary alluaudite (*yellowish*). Plane polarized light. The long edge of the photograph is approximately 5 mm. **c** Primary alluaudite (*orange*) + fillowite (*light gray*) assemblage form the Kabira pegmatite, Uganda. It is important to note the absence of reaction texture at the grain boundary between these two phosphates. Transmitted light, crossed polars. The long edge of the photograph is approximately 2.5 mm. **d** Hagendorfite from the Hagendorf-Süd pegmatite, Germany (*green*), associated with lamellae of hematite (*deep red and black*). Plane polarized light. The long edge of the photograph is approximately 2.5 mm

fugacity than those controlled by the NNO buffer, or at a higher pressure than 1 kbar.

Influence of oxygen fugacity on the crystallization of primary Fe–Mn phosphates

Grains of hematite have been observed in hagendorfite and triphylite, in the Hagendorf-Süd pegmatite, Germany (Boury 1981; see Fig. 13d), whereas magnetite is associated with triplite, $(Mn,Fe^{2+})_2(PO_4)F$, and with ferrisicklerite, $Li_{1-x}(Fe^{3+},Mn^{2+})(PO_4)$, in the Clementine II pegmatite, Namibia (Keller et al. 1994). The occurrence of these iron oxides, in close association with the primary phosphates, particularly with hagendorfite, permits the estimation of the oxygen fugacity conditions which prevailed during pegmatite crystallization.

Magnetite indicates an oxygen fugacity which could correspond to that controlled by the NNO buffer, and hematite indicates an oxygen fugacity higher than that controlled by the HM buffer. This very high oxygen fugacity, which occurs in some granitic pegmatites, could explain the absence of marićite, because this mineral appears to be stable only under a low oxygen fugacity, as shown in Fig. 10. In these high-$f(O_2)$ pegmatites, the crystallization temperature of single-phase alluaudites could reach 700°C, as shown in Fig. 11a. It is noteworthy that the occurrence of an alluaudite + hematite paragenesis in Hagendorf-Süd does not necessarily indicate that an oxygen fugacity close to CT has been reached, as suggested by Fig. 11b. An excess of iron in the system could indeed induce the crystallization of hematite, under an oxygen fugacity between HM and CT.

The occurrence of marićite in the metamorphic nodules from the Big Fish River area, Yukon, Canada (Sturman et al. 1977), is probably due to the low oxygen fugacity prevailing in the metamorphic rocks during their formation (Robinson et al. 1992), as compared to that in pegmatite. Marićite has also been described in some meteoritic rocks by Johnson et al. (2000) and by Lauretta and Buseck (2000), thus confirming the role of this mineral as a low-$f(O_2)$ indicator.

Acknowledgments Many thanks are due to J. Wautier, F. Fontan, and P. de Parseval, who performed the electron microprobe analyses, as well as to T. Baller, M. Burchard, and T. Fockenberg, who helped us to use the hydrothermal laboratory of the Ruhr-University of Bochum, Germany. FH acknowledges the F.N.R.S. (Belgium) for a position of "Chargé de Recherches" and for grants 1.5.113.05.F and 1.5.098.06.F, as well as the Alexander von Humboldt Foundation (Germany) for a Fellowship at Bochum, during the 2004–2005 academic year.

References

Antenucci D (1992) Synthèse et cristallochimie de composés à structure alluaudite. Incidences dans les processus d'altération des phosphates Fe–Mn des pegmatites granitiques. PhD thesis, University of Liège, 259 p

Araki T, Moore PB (1981) Fillowite, $Na_2Ca(Mn,Fe)^{2+}{}_7(PO_4)_6$: its crystal structure. Am Mineral 66:827–842

Auernhammer M, Effenberger H, Hentschel G, Reinecke T, Tillmanns E (1993) Nickenichite, a new arsenate from the Eifel, Germany. Mineral Petrol 48:153–166

Baldwin JR, Von Knorring O (1983) Compositional range of Mn-garnet in zoned granitic pegmatites. Can Mineral 21:683–688

Boury P (1981) Comportement du fer et du manganèse dans les associations de phosphates pegmatitiques. Master thesis, University of Liège, 118 p

Bridson JH, Quinlan SE, Tremaine PR (1998) Synthesis and crystal structure of marićite and sodium iron(III) hydroxyphosphate. Chem Mater 10:763–768

Brunet F, Chopin C, Seifert F (1998) Phase relations in the MgO–P_2O_5–H_2O system and the stability of phosphoellenbergerite: petrological implications. Contrib Mineral Petrol 131:54–70

Burnham CW (1991) LCLSQ version 8.4, least-squares refinement of crystallographic lattice parameters. Dept Earth Planetary Sciences, Harvard University, 24 p

Černý P (1991) Rare-element granitic pegmatites. Part I: Anatomy and internal evolution of pegmatite deposits. Geosci Can 18(2):49–67

Černý P, Meintzer RE, Anderson AJ (1985) Extreme fractionation in rare-element granitic pegmatites: selected examples of data and mechanisms. Can Mineral 23:381–421

Černý P, Ercit TS, Vanstone PT (1996) Petrology and mineralization of the Tanco rare-element pegmatite, Southeastern Manitoba. Field trip guidebook A4, Geological Association of Canada/Mineralogical Association of Canada Annual Meeting, Winnipeg, Manitoba, May 27–29, 1996, 63 p

Engel G (1976) Untersuchungen zur Kristallchemie verschiedener Phosphate $NaM^{II}PO_4$ und verwandter Verbindungen. N Jb Mineral Abh 127(2):197–211

Eugster HP (1957) Heterogeneous reactions involving oxidation and reduction at high pressures and temperatures. J Chem Phys 26:1760–1761

Fontan F (1978) Etude minéralogique et essais expérimentaux sur des phosphates de fer et de manganèse des pegmatites des Jebilet (Maroc) et des Pyrénées (France). PhD thesis, Université Paul-Sabatier, Toulouse, 250 p

Fontan F, Huvelin P, Orliac M, Permingeat F (1976) La ferrisicklérite des pegmatites de Sidi-Bou-Othmane (Jebilet, Maroc) et le groupe des minéraux à structure de triphylite. Bull Soc française Minéral Cristall 99:274–286

Fransolet A-M (1975) Etude minéralogique et pétrologique des phosphates de pegmatites granitiques. PhD thesis, University of Liège, 333 p

Fransolet A-M (1977) Le problème génétique des alluaudites. Bull Soc française Minéral Cristall 100:348–352

Fransolet A-M, Abraham K, Speetjens J-M (1985) Evolution génétique et signification des associations de phosphates de la pegmatite d'Angarf-Sud, plaine de Tazenakht, Anti-Atlas, Maroc. Bull Minéral 108:551–574

Fransolet A-M, Keller P, Fontan F (1986) The phosphate mineral associations of the Tsaobismund pegmatite, Namibia. Contrib Mineral Petrol 92:502–517

Fransolet A-M, Antenucci D, Fontan F, Keller P (1994) New relevant data on the crystal chemistry, and on the genetical problem of alluaudites and wyllieites. In: Abstracts of the 16th IMA general meeting, Pisa, pp 125–126

Fransolet A-M, Keller P, Fontan F (1997) The alluaudite group minerals: their crystallochemical flexibility and their modes of formation in the granite pegmatites. In: Abstracts of the meeting "phosphates: biogenic to exotic", London

Fransolet A-M, Fontan F, Keller P, Antenucci D (1998) La série johnsomervilleite-fillowite dans les associations de phosphates de pegmatites granitiques de l'Afrique centrale. Can Mineral 36:355–366

Fransolet A-M, Hatert F, Fontan F (2004) Petrographic evidence for primary hagendorfite in an unusual assemblage of phosphate minerals, Kibingo granitic pegmatite, Rwanda. Can Mineral 42:697–704

Ginzbourg AI (1960) Specific geochemical features of the pegmatitic process. In: International Geological Congress, report of the 21st session, Norden, Part 17, pp 111–121

Hatert F (2002) Cristallochimie et synthèse hydrothermale d'alluaudites dans le système Na–Mn–Fe–P–O: contribution au problème de la genèse de ces phosphates dans les pegmatites granitiques. PhD thesis, University of Liège, 247 p

Hatert F (2004a) The crystal chemistry of lithium in the alluaudite structure: a study of the $(Na_{1-x}Li_x)_{1.5}Mn_{1.5}Fe^{3+}{}_{1.5}(PO_4)_3$ solid solution (x = 0 to 1). Mineral Petrol 81:205–217

Hatert F (2004b) Etude cristallochimique et synthèse hydrothermale des alluaudites: contribution nouvelle au problème génétique des phosphates de fer et de manganèse dans les pegmatites granitiques et, partant, à celui de l'évolution de ces gisements. Mém Acad royale Sci Belgique, Cl Sci, Coll in-8, 3ème série XXI: 96 p

Hatert F, Keller P, Lissner F, Antenucci D, Fransolet A-M (2000a) First experimental evidence of alluaudite-like phosphates with high Li-content: the $(Na_{1-x}Li_x)MnFe_2(PO_4)_3$ series (x = 0 to 1). Eur J Mineral 12:847–857

Hatert F, Fransolet A-M, Grandjean F, Long GJ (2000b) Solid state syntheses and crystal chemistry of phosphates in the Na_2O–MnO–Fe_2O_3–P_2O_5 system: preliminary results. J Conf Abstr 5:46

Hatert F, Antenucci D, Fransolet A-M, Liégeois-Duyckaerts M (2002) The crystal chemistry of lithium in the alluaudite structure: a study of the $(Na_{1-x}Li_x)CdIn_2(PO_4)_3$ solid solution ($x = 0$ to 1). J Solid State Chem 163:194–201

Hatert F, Hermann RP, Long GJ, Fransolet A-M, Grandjean F (2003) An X-ray Rietveld, infrared, and Mössbauer spectral study of the $NaMn(Fe_{1-x}In_x)_2(PO_4)_3$ alluaudite-like solid solution. Am Mineral 88:211–222

Hatert F, Long GJ, Hautot D, Fransolet A-M, Delwiche J, Hubin-Franskin MJ, Grandjean F (2004) A structural, magnetic, and Mössbauer spectral study of several Na–Mn–Fe-bearing alluaudites. Phys Chem Miner 31:487–506

Hatert F, Rebbouh L, Hermann RP, Fransolet A-M, Long GJ, Grandjean F (2005) Crystal chemistry of the hydrothermally synthesized $Na_2(Mn_{1-x}Fe^{2+}{}_x)_2Fe^{3+}(PO_4)_3$ alluaudite-type solid solution. Am Mineral 90:653–662

Héreng P (1989) Contribution à l'étude minéralogique de phosphates de fer et de manganèse de la pegmatite de Buranga, Rwanda. Master thesis, University of Liège, 101 p

Hermann RP, Hatert F, Fransolet A-M, Long GJ, Grandjean F (2002) Mössbauer spectral evidence for next-nearest neighbor interactions within the alluaudite structure of $Na_{1-x}Li_xMnFe_2(PO_4)_3$. Solid State Sci 4:507–513

Huvelin P, Orliac M, Permingeat F (1972) Ferri-alluaudite calcifère de Sidi-bou-Othmane (Jebilet, Maroc). Notes Serv géol Maroc 32(241):35–49

Johnson CL, Lauretta DS, Buseck P (2000) A high-resolution transmission electron microscopy study of fine-grained phosphates in metal from the Bishunpur LL3.1 ordinary chondrite. In: 63rd Annual Meteoritical Society Meeting, Chicago, Illinois, p 5303

Keller P, Von Knorring O (1989) Pegmatites at the Okatjimukuju farm, Karibib, Namibia. Part I: phosphate mineral associations of the Clementine II pegmatite. Eur J Mineral 1:567–593

Keller P, Fransolet A-M, Fontan F (1994) Triphylite–lithiophilite and triplite–zwieselite in granitic pegmatites: their textures and genetic relationships. N Jb Mineral Abh 168(2):127–145

Keller P, Hatert F, Lissner F, Schleid T, Fransolet A-M (2006) Hydrothermal synthesis and crystal structure of $Na(Na,Mn)_7Mn_{22}(PO_4)_{18}0.5H_2O$, a new compound of fillowite structure type. Eur J Mineral (in press)

Khorari S (1997) Cristallochimie des arséniates de structure alluaudite. PhD thesis, University of Liège

Lahti SI (1981) On the granitic pegmatites of the Eräjärvi area in Orivesi, southern Finland. Geol Surv Finland Bull 314:82

Lauretta DS, Buseck PR (2000) Chondrule formation and volatile recondensation recorded in an opaque assemblage from the Bishunpur chondrite. Lunar and Planetary Science XXXI, Houston, Texas, p 1136

Le Page Y, Donnay G (1977) The crystal structure of the new mineral marićite, $NaFePO_4$. Can Mineral 15:518–521

London D (1986) Magmatic-hydrothermal transition in the Tanco rare-element pegmatite: evidence from fluid inclusions and phase-equilibrium experiments. Am Mineral 71:376–395

London D, Wolf MB, Morgan GB, Gallego Garrido M (1999) Experimental silicate–phosphate equilibria in peraluminous granitic magmas, with a case study of the Alburquerque batholith at Tres Arroyos, Badajoz, Spain. J Petrol 40: 215–240

London D, Morgan GB, Wolf MB (2001) Amblygonite–montebrasite solid solutions as monitors of fluorine in evolved granitic and pegmatitic melts. Am Mineral 86:225–233

Mason B (1941) Minerals of the Varuträsk pegmatite. XXIII. Some iron–manganese phosphate minerals and their alteration products, with special reference to material from Varuträsk. Geol Fören Stockholm Förh 63:117–175

Moore PB (1971) Crystal chemistry of the alluaudite structure type: contribution to the paragenesis of pegmatite phosphate giant crystals. Am Mineral 56:1955–1975

Moore PB (1972) Natrophilite, $NaMnPO_4$, has ordered cations. Am Mineral 57:1333–1344

Moore PB, Ito J (1979) Alluaudites, wyllieites, arrojadites: crystal chemistry and nomenclature. Mineral Mag 43:227–235

Morgan GB, London D (1987) Alteration of amphibolic wallrocks around the Tanco rare-element pegmatite, Bernic Lake, Manitoba. Am Mineral 72:1097–1121

Moring J, Kostiner E (1986) The crystal structure of $NaMnPO_4$. J Solid State Chem 61:379–383

Norton FJ (1955) Dissociation pressures of iron and copper oxides. General Electric Research Laboratory Report, 55-R1–1248

O'Neill HSC (1988) Systems Fe–O and Cu–O: thermodynamic data for the equilibria Fe–''FeO'', $Fe–Fe_3O_4$, ''FeO''–Fe_3O_4, $Fe_3O_4–Fe_2O_3$, $Cu–Cu_2O$, and $Cu_2O–CuO$ from emf measurements. Am Mineral 73:470–486

O'Neill HSC, Pownceby MI (1993) Thermodynamic data from redox reactions at high temperatures. I. An experimental and theoretical assessment of the electrochemical method using stabilized zirconia electrolytes, with revised values for the Fe–''FeO'', Co–CoO, Ni–NiO and $Cu–Cu_2O$ oxygen buffers, and new data for the $W-WO_2$ buffer. Contrib Mineral Petrol 114:296–314

Quensel P (1937) Minerals of the Varuträsk Pegmatite. I. The lithium–manganese phosphates. Geol Fören Stockholm Förh 59(1):77–96

Quensel P (1940) Minerals of the Varuträsk Pegmatite. XVII. Further comments on the minerals varulite and alluaudite. Geol Fören Stockholm Förh 62(3):297–302

Quensel P (1957) The paragenesis of the Varuträsk pegmatite, including a review of its mineral assemblage. Arkiv för Mineralogi och Geologi 2(2):9–125

Redhammer GJ, Tippelt G, Bernroider M, Lottermoser W, Amthauer G, Roth G (2005) Hagendorfite $(Na,Ca)MnFe_2(PO_4)_3$ from type locality Hagendorf (Bavaria, Germany): crystal structure determination and ^{57}Fe Mössbauer spectroscopy. Eur J Mineral 17:915–932

Robinson GW, Velthuizen JV, Ansell HG, Sturman BD (1992) Mineralogy of the Rapid Creek and Big Fish River area, Yukon Territory. Mineral Rec 23(4):1–47

Roda E, Fontan F, Pesquera A, Velasco F (1996) The phosphate mineral association of the granitic pegmatites of the Fregeneda area (Salamanca, Spain). Mineral Mag 60:767–778

Roda Robles E, Fontan F, Pesquera Pérez A, Keller P (1998) The Fe–Mn phosphate associations from the Pinilla de Fermoselle pegmatite, Zamora, Spain: occurrence of kryzhanovskite and natrodufrénite. Eur J Mineral 10:155–167

Roda E, Pesquera A, Gil-Crespo PP, Torres-Ruiz J, Fontan F (2005) Origin and internal evolution of the Li–F–Be–B–P-bearing Pinilla de Fermoselle pegmatite (Central Iberian Zone, Zamora, Spain). Am Mineral 90:1887–1899

Solodovnikov SF, Klevtsov PV, Solodovnikova ZA, Glinskaya LA, Klevtsova RF (1998) Binary molybdates $K_4M^{2+}(MoO_4)_3$ (M^{2+} = Mg, Mn, Co) and crystal structure of $K_4Mn(MoO_4)_3$. J Struct Chem 39(2):230–237

Stefanidis T, Nord AG (1984) Structural studies of thortveitite-like dimanganese diphosphate, $Mn_2P_2O_7$. Acta Crystallogr C40:1995–1999

Sturman BD, Mandarino JA, Corlett MI (1977) Marićite, a sodium iron phosphate from the Big Fish River area, Yukon Territory, Canada. Can Mineral 15:396–398

Tsyrenova GD, Solodovnikov SF, Zolotova ES, Tsybikova BA, Bazarova ZG (2000) Phase formation in the $K_2O(K_2CO_3)$–CdO–MoO_3 system. Russ J Inorg Chem 45(1):103–108

Tuttle OF (1949) Two pressure vessels for silicate–water studies. Geol Soc Am Bull 60:1727–1729